Chemometrics and Intelligent Laboratory Systems 240 (2023) 104910

Contents lists available at ScienceDirect

Chemometrics and Intelligent Laboratory Systems

journal homepage: www.elsevier.com/locate/chemometrics

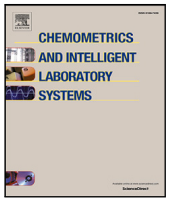

# Statistical analysis of randomized pseudo-first/second order kinetic models. Application to study the adsorption on cadmium ions onto tree fern

J.-C. Cortés [a], A. Navarro-Quiles [b], F.-J. Santonja [b], S.-M. Sferle [a,*]

[a] Instituto Universitario de Matemática Multidisciplinar, Universitat Politècnica de València, Camino de Vera s/n, 46022, Valencia, Spain
[b] Department of Statistics and Operational Research Universitat de València, Dr. Moliner 50, 46100, Burjassot, Spain

ARTICLE INFO

*Keywords:*
Pseudo-first order random kinetic model
Pseudo-second order random kinetic model
Probability density function
Random variable transformation technique
Real data
Estimation parameter techniques

ABSTRACT

Adsorption kinetics are commonly modeled using pseudo-first order (PFO) and pseudo-second order (PSO) rate laws. Both models are formulated via differential equations whose coefficients are commonly treated as deterministic quantities, which are calculated from experimental data using regression techniques. In this paper, we propose a full randomization of both models by assuming that all the parameters of the PFO and PSO models are random variables with arbitrary densities. Then, we probabilistically solve both models by determining semi-explicit expressions of the first probability density functions of the corresponding solution stochastic processes, as well as the densities of the time until a fixed adsorbed amount of reactant has been reached for each model too. The analysis is conducted under very general assumptions and is based on extensive application of the so-called Random Variable Transformation (RVT) technique. Finally, we apply all the aforementioned theoretical findings to model the adsorption of cadmium ions onto tree fern, using real data. We compare the results obtained by the randomized PFO and PSO models, using a Bayesian and a randomized version of the least mean square method to assign reasonable densities to model parameters. After comparing the results, the PSO model is selected, and, we then show how the RVT technique can be applied to obtain further key information, such as the second probability density function, of the solution and the covariance function.

## 1. Preliminaries

All chemical reactions take place at a rate that depends on conditions such as temperature, pressure, catalyst, concentration of the reacting substances, radiation, etc. The area of reaction kinetics focuses on the study of the rates of chemical reactions and the influence of the above-mentioned conditions on the rates. It is well established that the rate of a chemical reaction is directly proportional to the concentrations of the reacting substances since they are continuously consumed in the course of the reaction. As their concentrations decrease steadily, the rate of the reaction must vary over time, becoming the process slower as the reactants are used up. It is known that rate equations of chemical reactions can be conveniently represented via first-order differential equations whose right-hand side is mainly a linear or quadratic function of the difference between adsorption capacity at the equilibrium and the adsorption capacity at any previous time instants [1], [2, Ch. 7]. Below we specify some contributions where the adsorption chemical process is modeled via these two types of differential equations, which are usually referred to as kinetics models. It is worth pointing out that alternative approaches have also been considered to describe the dynamics of adsorption phenomena as Markovian processes [3], adaptive neuro-fuzzy inference systems [4], artificial neural networks [5], etc.

Adsorption is defined as the deposition or adhesion of molecular species (atoms, ions, or molecules) onto a surface. The adsorption method has important applications, for example, it is widely used in water and wastewater treatment processes [6–9]. There exist numerous mathematical models that describe the interactions between adsorbents and adsorbates at the equilibrium. The most extended models are the Lagergren or Ho models for pseudo-first order (PFO) and pseudo-second order (PSO), [10,11]. The PFO model is defined by the Lagergren equation

$$\frac{\mathrm{d}q(t)}{\mathrm{d}t} = k_1(q_\mathrm{e} - q(t)), \tag{1}$$

being $q_\mathrm{e}$ the adsorption capacity at equilibrium (mg/g), $q(t)$ the adsorption capacity at time $t$ (mg/g), and $k_1 > 0$ the speed constant ($\mathrm{min}^{-1}$).

* Corresponding author.
*E-mail addresses:* jccortes@imm.upv.es (J.-C. Cortés), ana.navarro@uv.es (A. Navarro-Quiles), francisco.santonja@uv.es (F.-J. Santonja), smsferle@doctor.upv.es (S.-M. Sferle).

https://doi.org/10.1016/j.chemolab.2023.104910
Received 16 January 2023; Received in revised form 17 May 2023; Accepted 28 June 2023
Available online 3 July 2023

The driving force of the process is $q_e - q(t)$, i.e. the vacant and accessible active centers on the adsorbent surface. On the other hand, the equation of the PSO model is

$$\frac{dq(t)}{dt} = k_2(q_e - q(t))^2, \tag{2}$$

where $k_2 > 0$ is the speed constant (g/mg min$^{-1}$). Both models have been extensively applied, see [9,12–16]. A review of the application of both models in the literature, over the last decades, can be found in [17].

As previously indicated, the application of these kinetic models depends on certain experimental conditions, which are indirectly embedded through the model parameters, namely, the adsorption capacity at equilibrium, $q_e$, and the corresponding speed constant, $k_n$ ($n = 1, 2$). In practice, the nature of these parameters is uncertain rather than deterministic since they are taken as nominal values that are fixed from experimental data, so containing error measurements (epistemic uncertainty). Even more, if the chemical experiment is carefully repeated under exactly the same conditions, one also observes further discrepancies that cannot be attributed to error measurements only but more complex factors that happen at the atomic and molecular levels, which are not completely known [18–20]. This second source of uncertainty is commonly termed aleatoric uncertainty. These facts motivate that the PFO and PSO models are better formulated, taking into account the uncertainties involved in the chemical process (aleatoric uncertainty) and the measurement process in the laboratory (epistemic uncertainty).

It is important to point out that there are mainly two ways of considering uncertainties when dealing with differential equations. The first approach is based on the so-called Stochastic Differential Equations (SDEs), and the second one is formulated via Random Differential Equations (RDEs). As pointed out in [21, p. 96], the methods and techniques required to analyze SDEs and RDEs rigorously are distinctly different. Below, we detail the most distinctive characteristics of SDEs and RDEs. On the one hand, SDEs require considerable mathematical efforts for their treatment, such as Itô calculus, and one assumes that the uncertainty follows a specific pattern (typically Gaussian) that drives the corresponding SDE. On the other hand, in the setting of RDEs, uncertainty is directly assigned to each model parameter giving greater flexibility in the choice of appropriate probability distributions to quantify the uncertainty of the phenomena under study.

Under the SDE approach, uncertainties are driven by a stochastic process whose sample path behavior is highly irregular (e.g., non-differentiability). The so-called Itô-type SDEs are the most commonly used in applications (they are driven by the Wiener process whose trajectories are nowhere differentiable). The rigorous treatment of these SDEs requires the Itô Calculus, which notably differs from the classical Newton-Leibniz Calculus [22]. Itô-type SDEs can be naturally motivated from classical ordinary differential equations by means of the perturbation, via the so-called White noise, of some model parameters. This approach implicitly assumes that uncertainty is modeled via the Gaussian pattern (the Wiener process and the White noise are both Gaussian and also unbounded). Since the pioneering works by Gillespie [23–25], SDEs have been applied to model the dynamic of concentrations in chemical reactions. Although the approach proposed in this paper is based on RDEs, we want to point out some recent contributions related to the PFO and PSO models we will deal with throughout this paper. In [26], one shows that the stochastic counterpart of the PFO model is a linear SDE with additive noise whose solution is the Ornstein–Uhlenbeck (OU) stochastic process, and afterward, authors propose a transformation of the OU process to formulate a stochastic general kinetic model which includes the PSO version to describe the approach to equilibrium and the variability inherent in experimental adsorption kinetics. In [27], one studies the sharp connection between the stochastically perturbed Keizer's model, which belongs to the PSO-type models, and its deterministic counterpart. Authors incorporate stochastic incidence into the classical Keizer's model and show that it may play a key role in the stochastic formulation for irreversible biochemical reactions.

Complementary to SDEs, RDEs permit treating each model parameter (initial/boundary conditions, forcing term and/or coefficients) as a random variable or a stochastic process rather than representing uncertainties driven via stochastic processes having specific distributions and properties (as Gaussianity or unboundedness as it happens with the White noise in the setting of SDEs) which might be unrealistic and hence limiting their applicability. As pointed out in the extant literature [28], this approach gives more flexibility to RDEs than SDEs to assign different types of probability distributions to model parameters, so allowing for better capturing uncertainties when dealing with real-world problems in different areas such as biology, chemistry, engineering, etc. As pointed out in [29, p. 258], the theory and application for RDEs are much less advanced than that for SDEs, so its development is currently an active field of research.

In this paper, we shall study the randomized versions of the PFO and PSO models (1) and (2), respectively, that can be compactly written as the following RDE

$$\frac{dq(t,\omega)}{dt} = k_n(\omega)(q_e(\omega) - q(t,\omega))^n, \qquad n = 1, 2, \quad \omega \in \Omega. \tag{3}$$

Hereinafter, we will assume that their model parameters, $q_e(\omega)$ and $k_n(\omega)$, are absolutely continuous random variables defined in a common complete probability space $(\Omega, \mathcal{F}_\Omega, \mathbb{P})$. For the sake of generality when developing our theoretical findings, henceforth we assume that $q_e(\omega)$ and $k_n(\omega)$ have a joint probability density function (PDF), say $f_0^n(k_n, q_e)$. In case of independence, this joint PDF can be factorized as the product of the corresponding marginals PDF, $f_0^n(k_n, q_e) = f_{k_n}(k_n) f_{q_e}(q_e)$.

The main goal of this paper is to probabilistically solve the randomized PFO and PSO models. As it shall see in detail later on, this goal will be achieved by taking advantage of their explicit solutions given by the following parametric stochastic process

$$q(t,\omega) = q_e(\omega)\left(1 - e^{-k_1(\omega)t}\right), \qquad \omega \in \Omega, \tag{4}$$

and

$$q(t,\omega) = \frac{k_2(\omega) q_e(\omega)^2 t}{1 + k_2(\omega) q_e(\omega) t}, \qquad \omega \in \Omega, \tag{5}$$

respectively.

In the setting of Uncertainty Quantification, solving probabilistically a model formulated via a differential equation means determining the main statistical properties of the model. In many contributions, the goal is just to determine the mean and the variance, which can be enough when dealing with a one-dimensional Gaussian model. Here, we go further and we face the computation of the so-called first probability density (1-PDF), denoted by $f_1(q,t)$, of the solution stochastic process $q(t,\omega)$ [30, Ch. 3]. The calculation of 1-PDF is advantageous since it provides a full probabilistic description of the solution at each time instant. In addition, all the one-dimensional statistical moments of $q(t,\omega)$ can be computed by integrating the 1-PDF,

$$\mathbb{E}\left[q(t,\omega)^m\right] = \int_{-\infty}^{\infty} q^m f_1(q,t)\, dq, \qquad m = 1, 2, \ldots, \tag{6}$$

where $\mathbb{E}[\cdot]$ denotes the expectation operator. In particular, one can obtain the mean

$$\mu_q(t) = \mathbb{E}\left[q(t,\omega)\right] = \int_{-\infty}^{\infty} q f_1(q,t)\, dq, \tag{7}$$

and the variance,

$$\sigma_q^2(t) = \mathbb{V}\left[q(t,\omega)\right] = \int_{-\infty}^{\infty} q^2 f_1(q,t)\, dq - \mu_q(t)^2. \tag{8}$$

Additionally, the 1-PDF permits calculating the probability that the solution lies within any particular interval of interest $[a, b]$, at every

time instant,

$$\mathbb{P}\left[\{\omega \in \Omega \ : \ a \le q(t,\omega) \le b\}\right] = \int_a^b f_1(q,t)\,\mathrm{d}q,$$

As well as, the probability that the adsorbed amount exceeds a given level, say $\hat{q}$,

$$\mathbb{P}\left[\{\omega \in \Omega \ : \ q(t,\omega) > \hat{q}\}\right] = \int_{\hat{q}}^{\infty} f_1(q,t)\,\mathrm{d}q,$$

which is often of specific interest when studying chemical reactions.

The paper is organized as follows. In Section 2, the 1-PDF of the solution stochastic processes for both randomized models, PFO and PSO are determined. Additionally, in this section, we compute, for both models, the density of a relevant quantity when dealing with kinetic reactions, the time needed to reach a particular level of adsorbed amount. In Section 3, we apply the theoretical results obtained in Section 2 to real data corresponding to the adsorption of cadmium onto ground-up tree fern and show a comparative analysis between the PFO and the PSO models, showing the latter better measures of goodness-of-fit. Then, additional key probabilistic information of the PSO model, such as the 2-PDF and the covariance function, are calculated. Finally, conclusions are drawn in Section 4.

## 2. Probabilistic solution via the 1-PDF of PFO and PSO kinetic models

This section is addressed to determine the 1-PDFs of the solution stochastic processes for the PFO and the PSO models. As it shall be seen later, we will obtain semi-explicit expressions in both cases that are very useful in practice, as illustrated in Section 3. Additionally, we will introduce a key random variable that describes the time associated with a specific adsorbed amount, and we will determine its PDF. To achieve these goals, we will take extensive advantage of the Random Variable Transformation (RVT) technique. This method permits calculating the joint PDF of a random vector which is obtained by mapping, via a one-to-one transformation, another random vector whose joint PDF is known.

**Theorem 1** (*RVT Technique [30]*). *Let* $\mathbf{u}(\omega) = (u_1(\omega), \dots, u_n(\omega))$ *and* $\mathbf{v}(\omega) = (v_1(\omega), \dots, v_n(\omega))$ *be n-dimensional absolutely continuous random vectors defined in a complete probability space* $(\Omega, \mathcal{F}_\Omega, \mathbb{P})$, *where* $\omega \in \Omega$. *Let* $\mathbf{r} : \mathbb{R}^n \to \mathbb{R}^n$ *be a one-to-one transformation of* $\mathbf{u}$ *into* $\mathbf{v}$, *i.e.,* $\mathbf{v} = \mathbf{r}(\mathbf{u})$. *Assume that* $\mathbf{r}$ *is continuous in* $\mathbf{u}$ *and has continuous partial derivatives with respect to* $\mathbf{u}$. *Then, if* $f_{\mathbf{U}}(\mathbf{u})$ *denotes the joint PDF of vector* $\mathbf{u}(\omega)$, *and* $\mathbf{s} = \mathbf{r}^{-1} = (s_1(v_1, \dots, v_n), \dots, s_n(v_1, \dots, v_n))$ *represents the inverse mapping of* $\mathbf{r} = (r_1(u_1, \dots, u_n), \dots, r_n(u_1, \dots, u_n))$, *the joint PDF of vector* $\mathbf{v}(\omega)$ *is given by*

$$f_{\mathbf{V}}(\mathbf{v}) = f_{\mathbf{U}}\left(\mathbf{s}(\mathbf{v})\right)\left|J_n\right|,$$

*where* $|J_n|$ *is the absolute value of the Jacobian, which is defined by*

$$J_n = \det\left(\frac{\partial \mathbf{s}}{\partial \mathbf{v}}\right) = \det\begin{pmatrix} \frac{\partial s_1(v_1,\dots,v_n)}{\partial v_1} & \cdots & \frac{\partial s_n(v_1,\dots,v_n)}{\partial v_1} \\ \vdots & \ddots & \vdots \\ \frac{\partial s_1(v_1,\dots,v_n)}{\partial v_n} & \cdots & \frac{\partial s_n(v_1,\dots,v_n)}{\partial v_n} \end{pmatrix}.$$

**Remark 1.** It is worth pointing out that the calculation of the 1-PDF can also be attacked using other techniques apart from the RVT method. For example, the so-called Liouville-Gibbs theorem [30, Ch. 6] states a partial differential equation (PDE) satisfied for the 1-PDF of the solution of a RDE. Solving exactly this PDE is exceptional, so, in general, one must rely on numerical methods that provide approximations of the 1-PDF. In contrast, as it shall be seen later, applying the RVT technique enables us to obtain semi-explicit (in terms of integrals) exact expressions of the 1-PDF, which is more advantageous. This justifies that we have chosen the RVT method in our subsequent analysis.

### 2.1. 1-PDFs of the solution stochastic processes of the PFO and PSO models

To determine the 1-PDF of the PFO model, we first fix $t > 0$, and apply Theorem 1 will the following notational identification, $\mathbf{u}(\omega) = (k_1(\omega), q_e(\omega))$ and $\mathbf{v}(\omega) = (v_1(\omega), v_2(\omega))$. We then define the following bijective mapping $\mathbf{r} : \mathbb{R}^2 \to \mathbb{R}^2$, whose components, $r_1$ and $r_2$, are defined by

$$\begin{aligned} v_1 &= r_1(k_1, q_e) = k_1, \\ v_2 &= r_2(k_1, q_e) = q_e\left(1 - \mathrm{e}^{-k_1 t}\right), \end{aligned}$$

where notice that its second component is just the solution of the PFO model (see (4)). The components, $s_1$ and $s_2$, of its inverse mapping, $\mathbf{s} : \mathbb{R}^2 \to \mathbb{R}^2$, and the absolute value of its Jacobian, $|J|$, are respectively given by

$$\left.\begin{aligned} k_1 &= s_1(v_1, v_2) = v_1, \\ q_e &= s_2(v_1, v_2) = \frac{v_2\,\mathrm{e}^{v_1 t}}{\mathrm{e}^{v_1 t} - 1}, \end{aligned}\right\} \qquad |J| = \frac{\mathrm{e}^{v_1 t}}{\mathrm{e}^{v_1 t} - 1} > 0,$$

since $v_1 = k_1 > 0$ and $k_1(\omega) > 0$, for all $\omega \in \Omega$. Therefore, according to Theorem 1, the joint PDF of the random vector $(v_1(\omega), v_2(\omega))$ is

$$f_{v_1,v_2}(v_1, v_2) = f_0^1\left(v_1, \frac{v_2\,\mathrm{e}^{v_1 t}}{\mathrm{e}^{v_1 t} - 1}\right)\frac{\mathrm{e}^{v_1 t}}{\mathrm{e}^{v_1 t} - 1}, \tag{9}$$

where recall that $f_0^1(k_1, q_e)$ denotes the joint PDF of the initial random parameters $(k_1(\omega), q_e(\omega))$. Then, the 1-PDF of the solution stochastic process of the PFO model, $q(t,\omega)$, is obtained by marginalizing expression (9),

$$\text{PFO}: \quad f_1(q,t) = \int_0^\infty f_0^1\left(k_1, \frac{q\,\mathrm{e}^{k_1 t}}{\mathrm{e}^{k_1 t} - 1}\right)\frac{\mathrm{e}^{k_1 t}}{\mathrm{e}^{k_1 t} - 1}\,\mathrm{d}k_1. \tag{10}$$

Notice that this expression is semi-explicit since it depends on the calculation of an integral. In the particular case that $k_1(\omega)$ and $q_e(\omega)$ are independent, this expression writes

$$\text{PFO}: \quad f_1(q,t) = \int_0^\infty f_{k_1}(k_1) f_{q_e}\left(\frac{q\,\mathrm{e}^{k_1 t}}{\mathrm{e}^{k_1 t} - 1}\right)\frac{\mathrm{e}^{k_1 t}}{\mathrm{e}^{k_1 t} - 1}\,\mathrm{d}k_1, \tag{11}$$

where $f_{k_1}$ and $f_{q_e}$ denote the PDFs of $k_1(\omega)$ and $q_e(\omega)$, respectively.

Now, we determine the 1-PDF of the solution stochastic process corresponding to the PSO model. Again, we will take advantage of the RVT technique. Let $t > 0$ be a fixed time instant and we define the one-to-one mapping $\mathbf{r} : \mathbb{R}^2 \to \mathbb{R}^2$,

$$\begin{aligned} v_1 &= r_1(k_2, q_e) = \frac{k_2 q_e^2 t}{1 + k_2 q_e t}, \\ v_2 &= r_2(k_2, q_e) = q_e. \end{aligned}$$

The inverse mapping, $\mathbf{s} : \mathbb{R}^2 \to \mathbb{R}^2$, of $\mathbf{r}$ is obtained by isolating $k_2$ in the first component,

$$\begin{aligned} k_2 &= s_1(v_1, v_2) = \frac{v_1}{v_2(v_2 - v_1)t}, \\ q_e &= s_2(v_1, v_2) = v_2. \end{aligned}$$

And, the absolute value of the Jacobian of the inverse mapping $\mathbf{s}$ is

$$|J| = \frac{1}{(v_2 - v_1)^2 t} > 0.$$

Observe that the inverse mapping is well defined,

$$v_2 - v_1 = q_e - \frac{k_2 q_e^2 t}{1 + k_2 q_e t} = \frac{q_e}{1 + k_2 q_e t} > 0,$$

since $t > 0$ and $k_2(\omega) > 0$ and $q_e(\omega) > 0$ for all $\omega \in \Omega$. Therefore, by Theorem 1 the PDF of random vector $\mathbf{v}(\omega) = \left(q(t,\omega), q_e(\omega)\right)$ can be expressed, in terms of the known joint PDF $f_0^2(k_2, q_e)$, as follows

$$f_{v_1,v_2}(v_1, v_2) = f_0^2\left(\frac{v_1}{v_2(v_2 - v_1)t}, v_2\right)\frac{1}{(v_2 - v_1)^2 t}.$$

Finally, marginalizing this expression with respect to the random variable $v_2(\omega) = q_e(\omega)$, and taking $t > 0$ arbitrary, the 1-PDF of the solution stochastic process, $q(t, \omega)$, given in (5), is

$$\text{PSO:} \quad f_1(q,t) = \int_0^\infty f_0^2\left(\frac{q}{q_e(q_e-q)t}, q_e\right)\frac{1}{(q_e-q)^2 t}\,\mathrm{d}q_e. \tag{12}$$

Analogously as for the PFO, in the particular case that $k_2(\omega)$ and $q_e(\omega)$ are independent random variables, the above expression can be expressed as

$$\text{PSO:} \quad f_1(q,t) = \int_0^\infty f_{k_2}\left(\frac{q}{q_e(q_e-q)t}\right) f_{q_e}(q_e)\frac{1}{(q_e-q)^2 t}\,\mathrm{d}q_e, \tag{13}$$

where $f_{k_2}$ and $f_{q_e}$ denote the PDFs of $k_2(\omega)$ and $q_e(\omega)$, respectively.

**Remark 2.** We must highlight that the transformation chosen to apply Theorem 1 is not unique. The variable that we know how to isolate is chosen and leaving the rest as the identity. In this manner, we ensure the existence of the inverse, and the Jacobian is easily calculated. It can be seen that the choice of a proper mapping is a key point. Indeed, in [31], one illustrates through some models that the final expression for the 1-PDF can become computationally costly depending on the transformation we have defined when applying the RVT method.

### 2.2. PDF of the time, $t(\omega)$, to reach a fixed adsorbed amount

A key question when dealing with kinetics models formulated via SDEs and RDEs is to determine when the reaction has consumed a specific level of a reactant (see, for instance, [26,32], respectively). As in the setting of RDEs, the model parameters are random variables, the answer to this question is not a number but a random variable, and the fullest way to answer this interesting issue is to obtain the PDF of such a random variable. In this section, we answer this problem for both models, PFO and PSO, in terms of the PDF of the random vector $(q_e(\omega), k_n(\omega))$ under very general hypotheses. If $\rho_q > 0$ denotes the adsorbed amount of reactant, then from (4) is clear that

$$\text{PFO}: \quad t(\omega) = \frac{1}{k_1(\omega)}\log\left(\frac{q_e(\omega)}{q_e(\omega)-\rho_q}\right), \qquad \omega \in \Omega. \tag{14}$$

Observe that the random variable $t(\omega)$ is well-defined if and only if it is positive for each $\omega \in \Omega$. Then, from expression (14), $t(\omega)$ is defined in the conditional probability space $(\Omega, \mathcal{F}_\Omega, \mathbb{P}[\cdot|C])$, where $C = \{\omega \in \Omega : q_e(\omega) - \rho_q > 0\} \in \mathcal{F}_\Omega$. Now, we fixed $\rho_q > 0$ and apply Theorem 1 to the following bijective mapping $\mathbf{r} : \mathbb{R}^2 \to \mathbb{R}^2$, that transforms the vector $\mathbf{u}(\omega) = \big(k_n(\omega), q_e(\omega),\big)$ into $\mathbf{v}(\omega) = (v_1(\omega), v_2(\omega))$, being

$$v_1 = r_1(k_1, q_e) = \frac{1}{k_1}\log\left(\frac{q_e}{q_e-\rho_q}\right),$$
$$v_2 = r_2(k_1, q_e) = q_e.$$

It is easy to check that the Jacobian is different from zero and compute the inverse mapping of $\mathbf{r}$. After some computations, we obtain the PDF of the time, which in the case of PFO model is given by

$$\text{PFO}: \quad f_t(t;\rho_q) = \frac{1}{t^2}\int_0^\infty f_0^1\left(\frac{1}{t}\log\left(\frac{q_e}{q_e-\rho_q}\right), q_e\right)\log\left(\frac{q_e}{q_e-\rho_q}\right)\mathrm{d}q_e. \tag{15}$$

This PDF is defined in the conditional probability space $(\Omega, \mathcal{F}_\Omega, \mathbb{P}[\cdot|C])$.

To determine the PDF of the time with regard to the random PSO model, first, observe from (5), that given a value of $\rho_q$, the random variable time is given by

$$\text{PSO:} \quad t(\omega) = \frac{\rho_q}{k_2(\omega)q_e(\omega)(q_e(\omega)-\rho_q)}, \qquad \omega \in \Omega. \tag{16}$$

Analogously as it has been explained for the PFO model, this random variable $t(\omega)$ is well-defined if and only if $q_e(\omega) - \rho_q > 0$, for each $\omega \in \Omega$, and then is defined in the same conditional probability space $(\Omega, \mathcal{F}_\omega, \mathbb{P}[\cdot|C])$ previously introduced. Then, we apply Theorem 1 to the following mapping, $\mathbf{r} : \mathbb{R}^2 \to \mathbb{R}^2$, that transforms $\mathbf{u} = (k_2, q_e)$ into $\mathbf{v} = (v_1, v_2)$,

$$v_1 = r_1(k_2, q_e) = \frac{\rho_q}{k_2 q_e(q_e-\rho_q)},$$
$$v_2 = r_2(k_2, q_e) = q_e.$$

The inverse mapping $\mathbf{s} = \mathbf{r}^{-1} : \mathbb{R}^2 \to \mathbb{R}^2$, is easily obtained by isolating $k_2$,

$$k_2 = s_1(v_1, v_2) = \frac{\rho_q}{v_1 v_2(v_2-\rho_q)},$$
$$q_e = s_2(v_1, v_2) = v_2.$$

The absolute value of the Jacobian of the inverse mapping $\mathbf{s}$ is

$$|J| = \frac{1}{v_1^2}\frac{\rho_q}{v_2(v_2-\rho_q)} > 0,$$

since $v_1 > 0$ and $v_2 - \rho_q = q_e - \rho_q > 0$ in the conditional space, $(\Omega, \mathcal{F}_\Omega, \mathbb{P}[\cdot|C])$, previously defined. Notice that $v_1$ is just the time (see expression (16)). Then, given a fixed $\rho_q$, according to Theorem 1, the PDF of the random vector $\mathbf{v}(\omega)$ is

$$f_{v_1,v_2}(v_1, v_2) = f_0^2\left(\frac{\rho_q}{v_1 v_2(v_2-\rho_q)}, v_2\right)\frac{1}{v_1^2}\frac{\rho_q}{v_2(v_2-\rho_q)}.$$

Marginalizing the last expression with respect to the last component of the random vector $\mathbf{v}(\omega)$, one obtains the PDF of the time, for a fixed $\rho_q$, in the conditional probability space $(\Omega, \mathcal{F}, \mathbb{P}[\cdot|C])$,

$$\text{PSO:} \quad f_t(t;\rho_q) = \int_0^\infty f_0^2\left(\frac{\rho_q}{tq_e(q_e-\rho_q)}, q_e\right)\frac{1}{t^2}\frac{\rho_q}{q_e(q_e-\rho_q)}\,\mathrm{d}q_e. \tag{17}$$

**Remark 3.** Similarly, as we have done for the 1-PDF of the solution stochastic processes of the PFO and PSO models (see expressions (11) and (13), respectively), we can particularize expressions (15) and (17) in the case that random variables $k_1$ and $q_e$ are independent in the PFO model, and $k_2$ and $q_e$ are independent in the PFO model as follows

$$\text{PFO}: \quad f_t(t;\rho_q) = \frac{1}{t^2}\int_0^\infty f_{k_1}\left(\frac{1}{t}\log\left(\frac{q_e}{q_e-\rho_q}\right)\right) f_{q_e}(q_e)\log\left(\frac{q_e}{q_e-\rho_q}\right)\mathrm{d}q_e, \tag{18}$$

where $f_{k_1}$ and $f_{q_e}$ denote the PDFs of $k_1(\omega)$ and $q_e(\omega)$, respectively.

$$\text{PSO:} \quad f_t(t;\rho_q) = \int_0^\infty f_{k_2}\left(\frac{\rho_q}{q_e(q_e-\rho_q)t}\right) f_{q_e}(q_e)\frac{1}{t^2}\frac{\rho_q}{q_e(q_e-\rho_q)}\,\mathrm{d}q_e, \tag{19}$$

where $f_{k_2}$ and $f_{q_e}$ denote the PDFs of $k_2(\omega)$ and $q_e(\omega)$, respectively.

**Table 1**
Adsorption capacity of cadmium ions onto tree fern, $q_i$, for different time instants $t_i$, $i \in \{1, 2, \ldots, 9\}$.
*Source:* Source [33].

| | | | | | |
|---|---|---|---|---|---|
| $t_i$ (min) | 0 | 4 | 5 | 10 | |
| $q_i$ (mg/g) | 0 | 7.172414 | 8.022989 | 9.724138 | |
| $t_i$ (min) | 15 | 20 | 30 | 45 | 60 |
| $q_i$ (mg/g) | 9.793103 | 10.551724 | 10.574713 | 11.103448 | 11.195402 |

## 3. Application to real data

In this section, we illustrate how the theoretical findings established in Section 2 can be applied to real data. The data collected in Table 1 shows the adsorption of cadmium ions onto tree fern. For further details about the chemical experiment see Ref. [33].

In order to apply the results obtained in Section 2, we first need to set an admissible joint PDF, $f_0^i(k_i, q_e)$, of model parameters, i.e., of the random vector $(k_i(\omega), q_e(\omega))$, $i = 1$ (for the PFO model) and $i = 2$ (for the PSO model). As this is a crucial step in practice, we will apply

two approaches, the first one is based on Bayesian techniques, while the second one is based on the randomization of the Least Mean Square (RLMS) method, which consists in minimizing a certain distance (mean square error) that will be specified later.

### 3.1. PFO model: Bayes and RLMS parameter estimation

*Bayesian estimation of model parameters.* We use the Bayesian approach to estimate the distribution of the random parameters $k_1(\omega)$ and $q_e(\omega)$. This approach solves the limitations of other traditional methods, such as the maximum likelihood principle and the least mean square method, which do not take into account the variability that is to be expected in the model parameters. The Bayesian framework is set up by assuming a probability model, $\pi(\mathbf{y}|\theta)$, for the observed or experimental data, $\mathbf{y}$, given the vector of unknown parameters, $\theta$, and a prior distribution for the unknown parameters, $\pi(\theta)$. Then, using Bayes's formula one obtains the posterior distribution of the parameters depending on the experimental data, $\pi(\theta|\mathbf{y})$. For more information about the theoretical foundations and applications of Bayesian estimation method, it can be seen, for instance, in Ref. [34]. In our problem, the amount of adsorbent, $q_i$ is strictly positive (see Table 1). Thus, we assume that these set of values are random variables that follow a Gamma distribution, whose mean is given by the solution of the model at each time instant $t_i$, i.e.,

$$q_i|\theta \sim \mathrm{Ga}(\alpha_i, \beta), \tag{20}$$

where $\beta > 0$ is the rate parameter and $\alpha_i > 0$ is the shape parameter. Then, from the definition of the expectation of a Gamma distribution, and according to the solution of the PFO model given in (4), one must satisfy

$$\mathbb{E}\left[q_i\right] = \frac{\alpha_i}{\beta} = q_e(1 - e^{-k_1 t_i}) \quad \Longrightarrow \quad \alpha_i = (q_e(1 - e^{-k_1 t_i}))\beta. \tag{21}$$

In the Bayesian model (20)–(21), $\theta(\omega) = (q_e(\omega), k_1(\omega), \beta(\omega))$ is the unknown vector of parameters, and we consider a Gamma distribution for the conditional density of the data given the vector $\theta(\omega)$ ($\pi(\mathbf{y}|\theta)$). The next step is to consider appropriate prior distributions for the parameters $q_e(\omega)$, $k_1(\omega)$ and $\beta(\omega)$, which allows us to include prior information about the parameters. Based on the literature, see [35] and the references therein, we know that $q_e(\omega)$ and $k_1(\omega)$ must be positive, and moreover the latter is always smaller than 1. Then, we choose the following non-informative distributions, taking into account the information about the range

$$q_e(\omega) \sim \mathrm{U}(0, 100), \quad k_1(\omega) \sim \mathrm{U}(0, 1), \quad \beta(\omega) \sim \mathrm{Ga}(0.01, 0.01).$$

Since $\beta$ is the rate parameter of the Gamma distribution and we only know that it is positive, a fairly common non-informative distribution for these cases where the rate parameter is unknown is another Gamma distribution centered at 1 and with fairly large variance. As it is known, Markov Chain Monte Carlo (MCMC) techniques are applied to calculate the posterior distribution of the model parameters. For this goal, we have used the free statistical software WinBUGS, which uses Gibbs sampling and Metropolis algorithm, to generate a Markov chain by sampling from full conditional distributions, [36–38]. We set 3 chains, 25000 iterations for each chain, and a burn-in period of 5000 iterations to assess the convergence of MCMC chains. Convergence of MCMC chains has been evaluated by examining the trace plots (see Fig. A.8, Appendix). Trace plot is useful to assess the convergence or lack thereof of the Markov chain. It is a visual approach to monitoring convergence, in order to observe that the Markov chains constructed by the MCMC algorithm have reached their stationary process. Thus, convergence occurs when Markov chains converge in distribution to the posterior distribution of interest. Let us recall that the stationary distribution of the Markov chains is the posterior density. Fig. A.8 shows a random scatter around a mean value and that the three chains were well mixed. WinBUGS automatically calculates the deviance quantity. It is defined as $-2\log(\pi(\mathbf{y}|\theta))$ [38, p. 140], and it serves as a Bayesian measure of fit. The right column in Fig. A.8 shows the posterior distribution of each parameter of the Bayesian model. These distributions have been determined using the non-parametric method called kernel density estimation [39]. The bandwidth values that WinBUGS used in each case to smooth the samples to produce density estimates are shown in the same plot. The sample size is represented by $N$, which is 20000 since we have considered 25000 iterations, 5000 of which were used for burn-in. To complete the statistical analysis, we have performed other convergence diagnostics using the `coda` package in R. Specifically, the graphical results for the Gelman and Rubin's convergence diagnostic are shown in Fig. A.9 (see Appendix). From this plot, we can observe that the potential scale reduction factor is close to 1 for all the estimated parameters. This fact indicates that MCMC sampling converges to the estimated posterior distribution for each parameter [34, p. 285]. Once we have obtained the PDFs, $f_{k_1}(k_1)$ and $f_{q_e}(q_e)$, by means of the Bayesian method, we can observe that there is a negative correlation between random variables $k_1(\omega)$ and $q_e(\omega)$ (see Fig. A.10 in Appendix). To account for this statistical dependence, we will construct the joint PDF, $f_0^1(k_1, q_e)$, of the random vector $(k_1(\omega), q_e(\omega))$ by applying the theory of copulas [40]. This means that $f_0^1(k_1, q_e)$ marginally behaves as $f_{k_1}(k_1)$ and $f_{q_e}(q_e)$, but considering the statistical dependence between $k_1(\omega)$ and $q_e(\omega)$. We will specifically apply the FGM (Farlie–Gumbel–Morgenstern) copula, which depends on a parameter, say $\xi$, that modulates this negative dependence [40,41]. In our calculations, we have taken $\xi = -0.6$. Computations have been carried out by Mathematica© Software [42].

*RLMS estimation of model parameters.* To apply this technique, we first need to assume specific parametric distributions for the model parameters $k_1(\omega)$ and $q_e(\omega)$. Taking into account the positiveness and boundedness of both random variables within the setting of our chemical application, we will assume that $k_1(\omega)$ has a Beta distribution with shape parameters $k_1^1 > 0$ and $k_1^2 > 0$, i.e., $k_1(\omega) \sim \mathrm{Be}(k_1^1; k_1^2)$, and $q_e(\omega)$ has a Gaussian distribution of parameters $\mu_{q_e}$ and $\sigma_{q_e} > 0$ truncated on the positive real numbers, i.e., $q_e(\omega) \sim \mathrm{N}_T(\mu_{q_e}; \sigma_{q_e})$, where $T = (0, +\infty)$ (hence observe that we implicitly assume that $\mu_{q_e} > 0$). The choice of some reasonable distributions is a critical point when applying the RLMS method to estimate model parameters since many possibilities may be reasonable, but a decision must be made. Our previous choice is consistent with the results that we have previously obtained by the Bayesian approach as well as the available information about the model parameters. Indeed, as it has been previously commented, it is known from the literature that the random parameter $k_1(\omega)$ lies between 0 and 1. Moreover, as we can observe in Fig. A.8 (see Appendix), the shape of the PDF of this parameter may follow a beta distribution for adequate values of its parameters. It motivates that a reasonable distribution for $k_1(\omega$ is $\mathrm{Be}(k_1^1; k_1^2)$, where $k_1^1 > 0$ and $k_1^2 > 0$ must be determined. In the case of $q_e(\omega)$, from the graphical representation of the trace plot and of the posterior distribution in Fig. A.8, we can observe that both have symmetric positive densities. Therefore, we made the decision of choosing a normal distribution truncated on the positive real numbers. For consistency with the Bayesian approach previously applied to perform the estimation of model parameters, we now determine the joint PDF of the random vector $(k_1(\omega), q_e(\omega))$ by applying the FGM copula with parameter $\xi = -0.6$. This copula will be denoted by $f_0^1(k_1, q_e; k_1^1, k_1^2, \mu_{q_e}, \sigma_{q_e})$ to emphasize the dependence on the parameters corresponding to the initial distributions. At this point, notice two facts, first, that these parameters $k_1^1$, $k_1^2$, $\mu_{q_e}$ and $\sigma_{q_e}$ need to be determined yet, and secondly, that the PDF of the stochastic solution process will depend on them, $q(t, \omega; k_1^1, k_1^2, \mu_{q_e}, \sigma_{q_e})$. These parameters are calculated by solving the following optimization program

$$\min_{k_1^1, k_1^2, \mu_{q_e}, \sigma_{q_e} > 0} \quad \sum_{i=1}^{9} \left(q_i - \mathbb{E}\left[q(t_i, \omega; k_1^1, k_1^2, \mu_{q_e}, \sigma_{q_e})\right]\right)^2, \tag{22}$$

where the values $q_i$, $i = 1, 2, \ldots, 9$, are collected in Table 1, and the expectation, $\mathbb{E}\left[q(t_i, \omega; k_1^1, k_1^2, \mu_{q_e}, \sigma_{q_e})\right]$, is calculated via (7), being

**Table 2**
Results of different heuristic methods implemented in Mathematica′ applied to the optimization problem (22) corresponding to the PFO model.

| Methods | Time in seconds (min) | Optimal values | | | | Error |
|---|---|---|---|---|---|---|
| | | $k_1^1$ | $k_1^2$ | $\mu_{q_e}$ | $\sigma_{q_e}$ | |
| Nelder–Mead | 505.1485 (8.42) | 117.899632 | 320.476332 | 10.693922 | 0.145774 | 1.020992 |
| Random Search | 428.56876 (7.14) | 117.113796 | 325.643579 | 10.671013 | 0.164020 | 1.040055 |
| Simulated Annealing | 777.560168 (12.96) | 113.131991 | 309.063337 | 10.686646 | 0.130588 | 1.021799 |

**Table 3**
Expectations ($\mu_q(t)$) and standard deviations ($\sigma_q(t)$) of the solution stochastic process of the random PFO model at every time instant, for both Bayes and RLMS approaches.

| | | $t=4$ | $t=5$ | $t=10$ | $t=15$ | $t=20$ | $t=30$ | $t=45$ | $t=60$ |
|---|---|---|---|---|---|---|---|---|---|
| Bayes | $\mu_q(t)$ | 7.1460 | 7.9914 | 9.9804 | 10.4876 | 10.6196 | 10.6640 | 10.6675 | 10.6676 |
| | $\sigma_q(t)$ | 0.445843 | 0.423805 | 0.290430 | 0.259239 | 0.261084 | 0.264852 | 0.265401 | 0.265419 |
| RLMS | $\mu_q(t)$ | 7.0333 | 7.8906 | 9.9508 | 10.4948 | 10.6399 | 10.6898 | 10.6938 | 10.6939 |
| | $\sigma_q(t)$ | 0.305580 | 0.294833 | 0.187270 | 0.145382 | 0.142650 | 0.145270 | 0.145755 | 0.145771 |

**Table 4**
Comparison of the root mean square error (RMSE) and the mean absolute percentage error (MAPE) using the Bayes and the RLMS techniques to determine the PDFs of the model parameters, $k_1(\omega)$ and $q_e(\omega)$ for the random PFO model.

| | RMSE | MAPE |
|---|---|---|
| Bayes | 0.338432 | 2.58% |
| RLMS | 0.336814 | 2.90% |

**Table 5**
Values of the probabilities $p$, $p_1$ and $p_2$, defined in (23) and (24), at the time instants $t_i$, $i \in \{2,\dots,9\}$, collected in Table 1. This corresponds to the random PFO model.

| | | $p$ | $p_1$ | $p_2$ |
|---|---|---|---|---|
| $t=4$ | Bayes | 0.9504 | 0.0316 | 0.0180 |
| | RLMS | 0.9492 | 0.0219 | 0.0289 |
| $t=5$ | Bayes | 0.9485 | 0.0308 | 0.0207 |
| | RLMS | 0.9493 | 0.0207 | 0.0300 |
| $t=10$ | Bayes | 0.9481 | 0.0247 | 0.0272 |
| | RLMS | 0.9492 | 0.0203 | 0.0305 |
| $t=15$ | Bayes | 0.9482 | 0.0256 | 0.0262 |
| | RLMS | 0.9488 | 0.0252 | 0.0260 |
| $t=20$ | Bayes | 0.9479 | 0.0261 | 0.0260 |
| | RLMS | 0.9493 | 0.0255 | 0.0252 |
| $t=30$ | Bayes | 0.9480 | 0.0261 | 0.0259 |
| | RLMS | 0.9505 | 0.0248 | 0.0247 |
| $t=45$ | Bayes | 0.9480 | 0.0260 | 0.0260 |
| | RLMS | 0.9500 | 0.0250 | 0.0250 |
| $t=60$ | Bayes | 0.9480 | 0.0260 | 0.0260 |
| | RLMS | 0.9500 | 0.0250 | 0.0250 |

$f_1(q,t)$ the expression given in (10), that by construction will depend on parameters $k_1^1$, $k_1^2$, $\mu_{q_e}$ and $\sigma_{q_e}$. Notice that the objective function in the optimization program is defined by the Euclidean distance between the data, $q_i$, and the expectation of the solution stochastic process. To carry out this optimization problem we have implemented different heuristic methods, implemented in Mathematica©, the results of which are shown in Table 2. These provide local optimal, hence the results are slightly different but consistent. Then, we have chosen the Nelder–Mead method since it gives the smallest error, obtaining the following optimal values

$$k_1^1 = 117.899632, \quad k_1^2 = 320.476332, \quad \mu_{q_e} = 10.693922, \quad \sigma_{q_e} = 0.145774.$$

*Results.* In Fig. 1, we show the 1-PDF of the solution stochastic process, $f_1(q,t)$, of the PFO model, at the time instants $t_i$, $i \in \{1,2,\dots,9\}$, listed in Table 1. We show the graphical representation of $f_1(q,t)$ obtained via the two approaches previously applied to estimate the PDF of the model parameters, $k_1(\omega)$ and $q_e(\omega)$, namely, the Bayesian and the RLMS methods. We can observe from these two graphical representations that the results obtained by means of both methods are similar, although the PDFs calculated applying the RLMS method are more leptokurtic (lower variability). This fact can be explained by the methodology we have applied. Indeed, when applying RLMS method, we first perform a deterministic fitting to obtain initial values for the parameters on which the distributions chosen for the model parameters depend on. This strategy stretches the search performed by the optimization algorithm to find the best parameters that minimize the objective (error) function utilized when applying the RLMS method. This provides accurate values for the fitting, which gives rise to tighter confidence intervals and, consequently, leptokurtic distributions. In contrast, the assignment of probability distributions according to the Bayesian approach begins with non-informative prior densities having a higher variance, which leads to probability distributions having slightly larger variability. This behavior is clearer observed in Fig. 2, where the real data, $q_i$, $i = 0,1,\dots,9$ (collected in Table 1), the expectation ($\mu_q$) and the expectation plus/minus 1.96 standard deviations ($\mu_q \pm 1.96\sigma_q$) have been plotted. To quantitatively reinforce these comments, in Table 3, we show the expectation and standard deviation values for each time instant. We can see how the expectation values increase until stabilizing around the value 10.7 and how, on the other hand, the values of the standard deviation decrease until stabilizing over time around 0.27, when applying the Bayes approach and 0.15 for the RLMS case, approximately. Furthermore, it can be seen that, indeed, the standard deviation is slightly greater when applying the Bayesian method while the expectation is very similar. In order to compare the results obtained by applying both methods, in Table 4, we show two measures of goodness-of-fit, the root mean square error (RMSE) and the mean absolute percentage error (MAPE). We can observe that these measures are quite similar for both Bayes and RLMS approaches, as expected.

The intervals plotted in Fig. 2 have been built using the following rule

$$p = \mathbb{P}\left[\{\omega \in \Omega : \ \mu_q(t) - 1.96\sigma_q(t) \le q(t,\omega) \le \mu_q(t) + 1.96\sigma_q(t)\}\right], \qquad (23)$$

where $p \approx 0.95$, at each $t = t_i$, $i = 2\dots,9$. In Table 5, we show the exact values of $p$ at every $t_i$. Observe that they are about 0.95. Additionally,

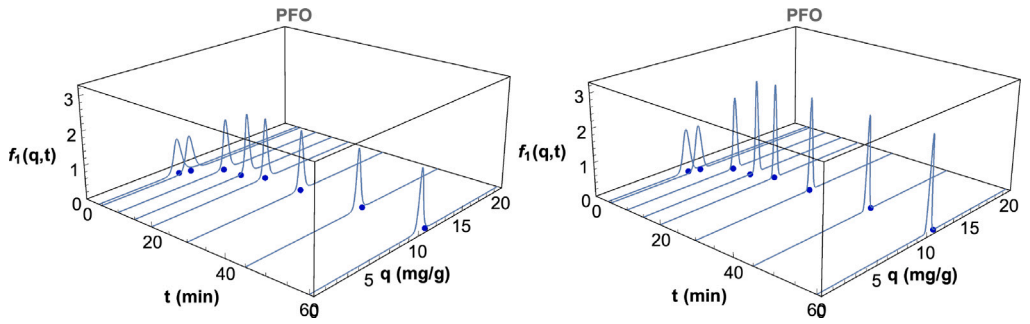


**Fig. 1.** Graphical representation of 1-PDF of the solution stochastic process of the random PFO model, $f_1(q,t)$, given in Eq. (10), at the time instants $t_i$, $i = 1,2,\ldots,9$, collected in Table 1. Left: The PDF of model parameters has been obtained using the Bayesian method. Right: The PDF of model parameters has been obtained using the RLMS method.

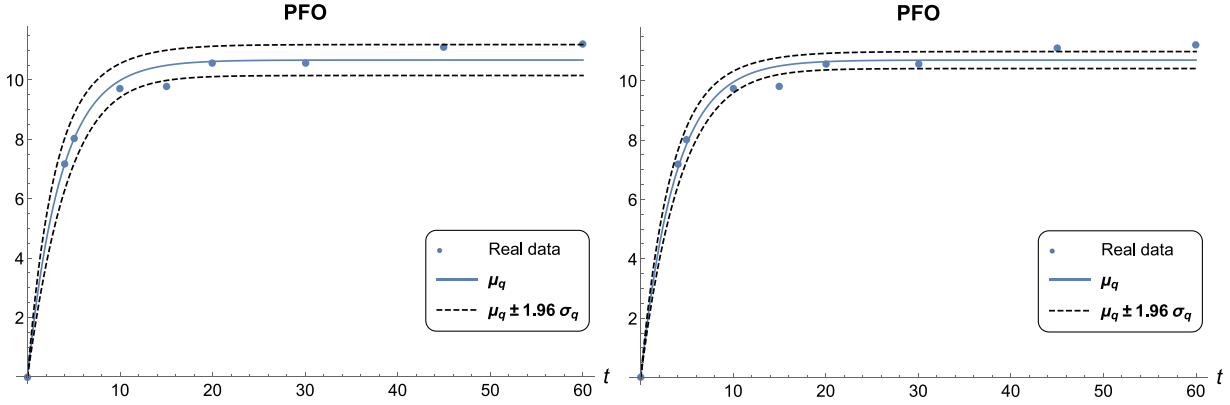


**Fig. 2.** Probabilistic fitting using the real data shown in Table 1 (points). The solid and dashed lines represent, respectively, the expectation ($\mu_q = \mu_q(t)$) and plus/minus 1.96 standard deviations ($\sigma_q = \sigma_q(t)$) of the solution stochastic process of the random PFO model (4). Calculations have been carried out with the PDFs obtained via the Bayes (left) and the RLMS (right) estimates for the PDFs of the model parameters, $k_1(\omega)$ and $q_e(\omega)$.

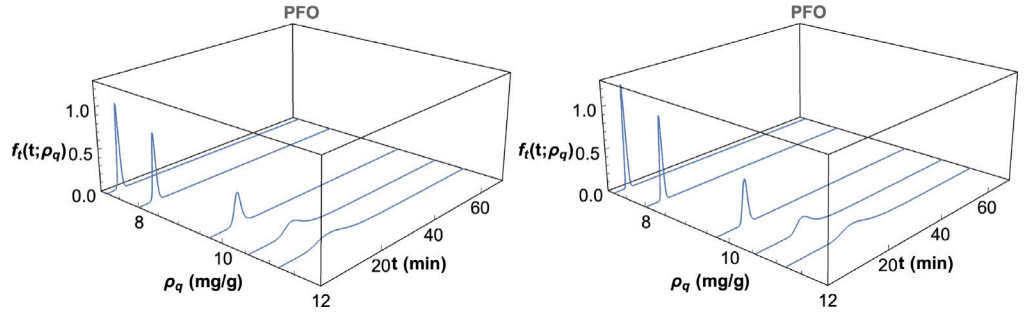


**Fig. 3.** PDF of the time, $f_t(t;\rho_q)$, for different fixed values of the adsorbed amount of reactant $\rho_q \in \{7.172, 8.023, 9.724, 10.575, 11.195\}$. Calculations have been carried out with the PDFs of the model parameters, $k_1(\omega)$ and $q_e(\omega)$, obtained via the Bayes (left) and RLMS (right) methods, in the context of the random PFO model.

in Table 5 we have included the following probabilities

$$\begin{aligned} p_1 &= \mathbb{P}\left[\{\omega \in \Omega : \ q(t,\omega) \geq \mu_q(t) + 1.96\sigma_q(t)\}\right], \\ p_2 &= \mathbb{P}\left[\{\omega \in \Omega : \ q(t,\omega) \leq \mu_q(t) - 1.96\sigma_q(t)\}\right], \end{aligned} \tag{24}$$

to highlight that the intervals are not symmetric with respect the mean $\mu_q(t)$, particularly for the first four time instants. This happens both when using the Bayes and the RLMS estimates obtained for the PDFs of the model parameters.

In Fig. 3, we show the PDF of the time, $t(\omega)$, until a given adsorbed amount of the chemical reactant, $\rho_q > 0$, is reached, for different values of $\rho_q \in \{7.172, 8.023, 9.724, 10.575, 11.195\}$, and using as PDFs of the model parameters $k_1(\omega)$ and $q_e(\omega)$ the ones obtained via the Bayes and RLMS methods. From these graphical presentations we can observe that both the expectation and the variability increase with $\rho_q$. Notice that slightly higher variability is obtained via the Bayes method. As indicated Section 2.2, the PDF, $f_t(t;\rho_q)$, has been calculated in the conditional probability space $(\Omega, \mathcal{F}_\Omega, \mathbb{P}[\cdot|C])$, being $C = \{\omega \in \Omega : q_e(\omega) - \rho_q > 0\}$, where the random variable, $t(\omega)$, is well-defined. In Table 6, the probability, $\mathbb{P}[C]$, of this event $C$ has been calculated, for the values of $\rho_q$ that have been previously indicated, via the Bayes and RLMS approaches. We complete the information collected in Table 6 with the values of the expectation and variance of $t(\omega)$. These statistics

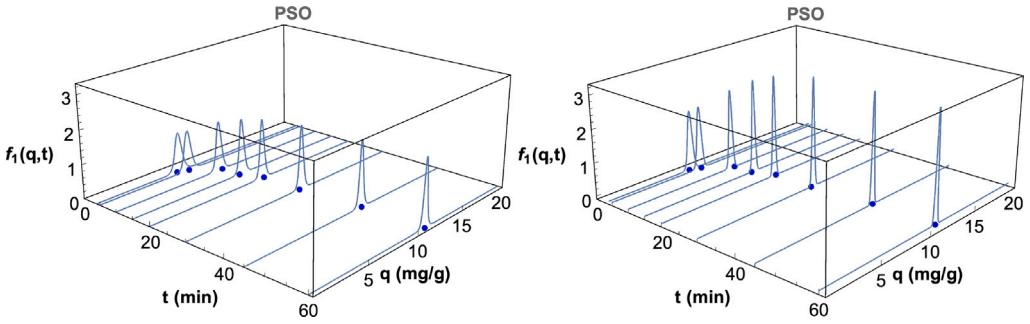


**Fig. 4.** Graphical representation of 1-PDF of the solution stochastic process of the random PSO model, $f_1(q,t)$, given in Eq. (12), at the time instants $t_i$, $i = 1,2,\ldots,9$, collected in Table 1. Left: The PDF of model parameters has been obtained using the Bayesian method. Right: The PDF of model parameters has been obtained using the RLMS method.

**Table 6**
Probability, $\mathbb{P}[C]$, of the event $C = \{\omega \in \Omega : q_e(\omega) - \rho_q > 0\}$ calculated in the context of the random PFO model, on the probability space $(\Omega, \mathcal{F}_\Omega, \mathbb{P})$. Expectation, $\mathbb{E}[t(\omega)|C]$, and variance, $\mathbb{V}[t(\omega)|C]$, of the time until a given amount of adsorbed amount of reactant, $\rho_q$, is reached. All the information has been calculated using the Bayes and RLMS approaches for different prefixed values of the chemical concentration, $\rho_q$.

| | $\rho_q \longrightarrow$ | 7.172 | 8.023 | 9.724 | 10.575 | 11.195 |
|---|---|---|---|---|---|---|
| $\mathbb{P}[C]$ | Bayes | 1 | 0.999987 | 0.997603 | 0.658030 | 0.025141 |
| | RLMS | 1 | 1 | 1 | 0.793255 | 0.000291 |
| $\mathbb{E}[t(\omega)\|C]$ | Bayes | 4.05 | 5.07 | 8.92 | 15.49 | 17.85 |
| | RLMS | 4.16 | 5.19 | 9.02 | 16.70 | 24.00 |
| $\mathbb{V}[t(\omega)\|C]$ | Bayes | 0.21 | 0.35 | 2.01 | 98.22 | 337.45 |
| | RLMS | 0.11 | 0.17 | 0.65 | 71.09 | 602.21 |

have been calculated using the PDF, given in formula (15), and $\mathbb{P}[C]$. For example, the expectation is calculated by

$$\mathbb{E}[t(\omega)|C] = \mathbb{E}\left[t(\omega)\mathbb{1}_C\right]/\mathbb{P}[C], \qquad \omega \in \Omega,$$

where $\mathbb{1}_C$ is the characteristic function for the event $C$. For example, according to Table 6, around 9 min are required to reach the adsorbed amount of reactant $\rho_q = 9.724$. Observe that the figures collected in this table, for the expectation and the variance, agree with the graphical behavior visualized in Fig. 3 in the sense that the mean and variance increase with $\rho_q$.

### 3.2. PSO model: Bayes and RLMS parameter estimation

In this subsection we perform a similar probabilistic analysis to the one shown in the previous section but for the random PSO model. Both methodologies Bayes and MC are applied to estimate the PDFs of the model input random variables, $k_2(\omega)$ and $q_e(\omega)$. From these marginal PDFs we construct the joint PDF using the FGM copula with parameter $\xi = -0.6$. The results will be presented following an analogous structure as for the PFO model, but avoiding the repetition of unnecessary details.

*Bayes parameter estimation.* Similarly as it has been done for the PFO model, we will first apply the Bayesian approach to estimate the marginal PDFs of the random parameters $k_2(\omega)$ and $q_e(\omega)$ for PSO model. We have chosen the Gamma distribution, with parameters $\alpha_i > 0$ and $\beta > 0$, for the data shown in Table 1 given the vector of unknown parameters $\boldsymbol{\theta}(\omega) = (q_e(\omega), k_2(\omega), \beta(\omega))$. In this case, given the expression of the solution of the PSO model, we have that

$$\mathbb{E}[q_i] = \frac{\alpha_i}{\beta} = \frac{k_2 q_e^2 t_i}{1 + k_2 q_e t_i} \quad \Longrightarrow \quad \alpha_i = \left(\frac{k_2 q_e^2 t_i}{1 + k_2 q_e t_i}\right)\beta. \tag{25}$$

For consistency with the study performed to model PFO, the prior distributions chosen for the random model parameters are the same,

$$q_e(\omega) \sim \mathrm{U}(0,100), \quad k_2(\omega) \sim \mathrm{U}(0,1), \quad \beta(\omega) \sim \mathrm{Ga}(0.01, 0.01).$$

In this case, we set 3 chains, 50000 iterations for each chain, and a burn-in period of 5000 iterations to assess the convergence of MCMC chains. Similarly, as the PFO model, the convergence of MCMC chains was evaluated by examining the trace plots in Fig. A.11 (see Appendix) and using the Gelman and Rubin's convergence diagnostic shown in Fig. A.12 (see Appendix). In this case, we also observe that the potential scale reduction factor is close to 1 for all the estimated parameters. Then, the MCMC sampling converges to the estimated posterior distribution for each parameter. In Fig. A.13 (see Appendix), we see that there is a negative correlation between the random parameters $q_e(\omega)$ and $k_2(\omega)$.

*RLMS estimation of model parameters.* In this case we consider that the RVs $k_2(\omega)$ and $q_e(\omega)$ have a parameter-dependent particular distributions. Once, for consistency with the study performed for the PFO model, we assume that $k_2(\omega)$ has a Beta distribution with shape parameters $k_2^1 > 0$ and $k_2^2 > 0$, $k_2(\omega) \sim \mathrm{Be}(k_2^1; k_2^2)$, and $q_e(\omega)$ has a Gaussian distribution truncated with mean, $\mu_{q_e}$, and standard deviation, $\sigma_{q_e}$, truncated on the positive real numbers, i.e. $q_e(\omega) \sim \mathrm{N}_T(\mu_{q_e}; \sigma_{q_e})$ being $T = (0, +\infty)$. The joint PDF, $f_0(q,t; k_1^1, k_1^2, \mu_{q_e}, \sigma_{q_e})$, is constructed using the FGM copula with parameter $\xi = -0.6$. The unknown parameters, $k_1^1$, $k_1^2$, $\mu_{q_e}$ and $\sigma_{q_e}$ are obtained solving the solution of optimization program (22) by considering $k_2^1$ and $k_2^2$ instead of $k_1^1$ and $k_1^2$, respectively. Based on Table 7 and the same reasons as in the previous case, we have obtained the following result

$$k_2^1 = 153.519698, \quad k_2^2 = 4033.860911, \quad \mu_{q_e} = 11.633311, \quad \sigma_{q_e} = 0.117726.$$

*Results.* In Fig. 4, we show the 1-PDF of the solution stochastic process of the PSO model obtained by applying the Bayes and the RLMS approaches. As it also happened for the PFO model and based on the same reasons, we can observe that the expectation obtained by both approaches is similar, while the variability is smaller via the RLMS method (the 1-PDF is more leptokurtic). In Table 8, we show the values of RMSE and the MAPE, being smaller these goodness-of-fit measures slightly smaller for the RLMS method. These figures are in agreement with the graphical results observed in Fig. 5, where we have plotted the expectation and the expectation plus/minus 1.96 standard deviations, using the Bayesian and the RLMS approaches. According to Table 9, these intervals have been constructed by (23) with $p \approx 0.95$, and, for the first time instants, they are not symmetric. Table 10 also shows that the values of the expectations are quite similar for each time instant and that they increase until reaching the equilibrium value, about 11.2, while the values of the standard deviations decrease until stabilizing at values 0.24, in the Bayes case, and 0.12, in the RLMS

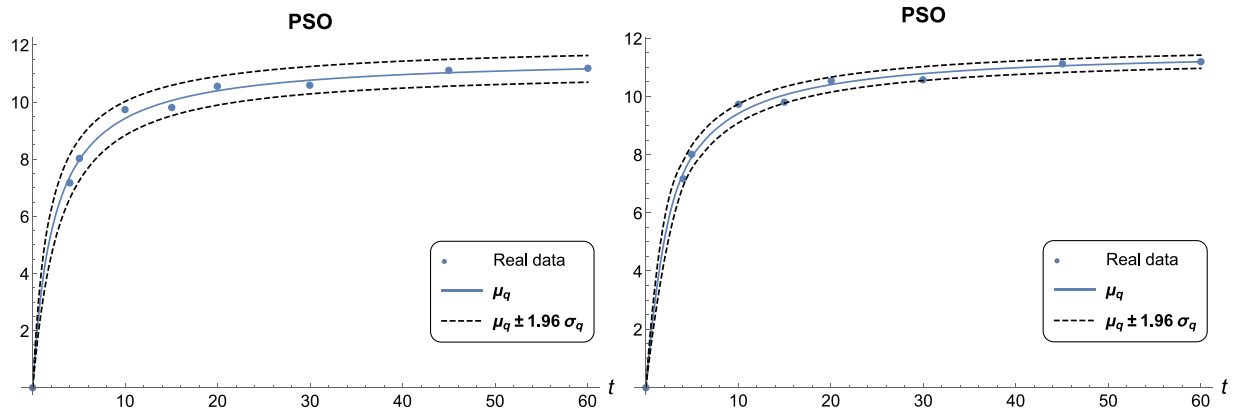


**Fig. 5.** Probabilistic fitting using real data shown in Table 1 (points). The solid and dashed lines represent, respectively, the expectation ($\mu_q = \mu_q(t)$) and plus/minus 1.96 standard deviations ($\sigma_q = \sigma_q(t)$) of the solution stochastic process of the random PFO model (5). Calculations have been carried out with the PDFs obtained via the Bayes (left) and the RLMS (right) estimates for the PDFs of the model parameters, $k_2(\omega)$ and $q_e(\omega)$.

**Table 7**
Results of different heuristic methods implemented in Mathematica′ applied to the optimization problem (22) corresponding to the PSO model.

| Methods | Time in seconds (min) | Optimal values | | | | Error |
|---|---|---|---|---|---|---|
| | | $k_1{}^1$ | $k_1{}^2$ | $\mu_{q_e}$ | $\sigma_{q_e}$ | |
| Nelder–Mead | 393.381492 (6.55) | 153.519698 | 4033.860911 | 11.633311 | 0.117726 | 0.267344 |
| Random Search | 344.929808 (5.75) | 153.751582 | 4063.047530 | 11.6216846 | 0.101027 | 0.271482 |
| Simulated Annealing | 644.124919 (10.74) | 148.605498 | 4028.554913 | 11.668446 | 0.120093 | 0.279787 |

**Table 8**
Comparison of the root mean square error (RMSE) and the mean absolute percentage error (MAPE) using the Bayes and the RLMS techniques to determine the PDFs of the model parameters, $k_1(\omega)$ and $q_e(\omega)$ in the random PSO model.

| | RMSE | MAPE |
|---|---|---|
| Bayes | 0.172720 | 1.71% |
| RLMS | 0.172351 | 1.65% |

**Table 9**
Values of the probabilities $p$, $p_1$ and $p_2$, defined in (23) and (24), at the time instants $t_i$, $i \in \{2, \ldots, 9\}$, collected in Table 1. This corresponds to the random PSO model.

| | | $p$ | $p_1$ | $p_2$ |
|---|---|---|---|---|
| $t = 4$ | Bayes | 0.9505 | 0.0290 | 0.0205 |
| | RLMS | 0.9490 | 0.0227 | 0.0285 |
| $t = 5$ | Bayes | 0.9509 | 0.0284 | 0.0207 |
| | RLMS | 0.9491 | 0.0224 | 0.0285 |
| $t = 10$ | Bayes | 0.9485 | 0.0268 | 0.0247 |
| | RLMS | 0.9493 | 0.0226 | 0.0281 |
| $t = 15$ | Bayes | 0.9486 | 0.0256 | 0.0258 |
| | RLMS | 0.9489 | 0.0237 | 0.0274 |
| $t = 20$ | Bayes | 0.9489 | 0.0248 | 0.0263 |
| | RLMS | 0.9489 | 0.0244 | 0.0267 |
| $t = 30$ | Bayes | 0.9490 | 0.0242 | 0.0268 |
| | RLMS | 0.9493 | 0.0249 | 0.0258 |
| $t = 45$ | Bayes | 0.9490 | 0.0239 | 0.0271 |
| | RLMS | 0.9501 | 0.0249 | 0.0250 |
| $t = 60$ | Bayes | 0.9490 | 0.0239 | 0.0271 |
| | RLMS | 0.9489 | 0.0256 | 0.0255 |

case, approximately. As it happens in the PFO model, the variability is smaller when applying the RLMS.

In Fig. 6, we show the PDF of the time until a given adsorbed amount of reactant $\rho_q \in \{7.172, 8.023, 9.724, 10.575, 11.195\}$ is reached. This PDF has been calculated in the conditional probability space $(\Omega, \mathcal{F}_\Omega, \mathbb{P}[\cdot|C])$. In Table 11, we collect the probability of the event $C$ and the conditional expectation and variability. From Fig. 6 and Table 11, we can observe that both the expectation and the variability increase when $\rho_q$ does. From Table 11, we can derive, for example, that around 12 min are required to adsorb $\rho_q = 9.724$ mg/g of reactant. This value differs with respect to the one provided by the PFO model, which was about 9 min only.

*Going further with the PSO model: computing the 2-PDF and the covariance.* Comparing the goodness-of-fit collected in Tables 4 and 8, we conclude that the PSO model provides better fitting. We have carefully revised recent literature about the PSO model, [43,44]. According to these contributions, the PSO model better reveals the adsorption mechanism at the active sites in most cases [43, p. 14], as it happens in our study case. From a theoretical perspective, this is justified because the PSO model is nonlinear, so taking better into account the complex dynamics often present in the adsorption process. Now, we will show how the RVT technique can be applied to obtain further probabilistic information about the solution corresponding to the PSO model. Specifically, we shall compute the 2-PDF, $f_2(q_1, t_1; q_2, t_2)$, of $q(t, \omega)$, i.e., the joint PDF of the solution at two arbitrary times instants, say $t_1$ and $t_2$. This two-dimensional PDF permits computing the covariance function, $\mathrm{Cov}_q(t_1, t_2)$

$$\mathrm{Cov}_q(t_1, t_2) = \mathbb{E}\left[q(t_1, \omega)q(t_2, \omega)\right] - \mathbb{E}\left[q(t_1, \omega)\right]\mathbb{E}\left[q(t_2, \omega)\right], \tag{26}$$

where

$$\mathbb{E}\left[q(t_1, \omega)q(t_2, \omega)\right] = \int_{\mathbb{R}^2} q_1 q_2 f_2(q_1, t_1; q_2, t_2)\,\mathrm{d}q_1\,\mathrm{d}q_2. \tag{27}$$

The covariance function provides a statistical measure of how much two variables change together. Furthermore, the covariance permits

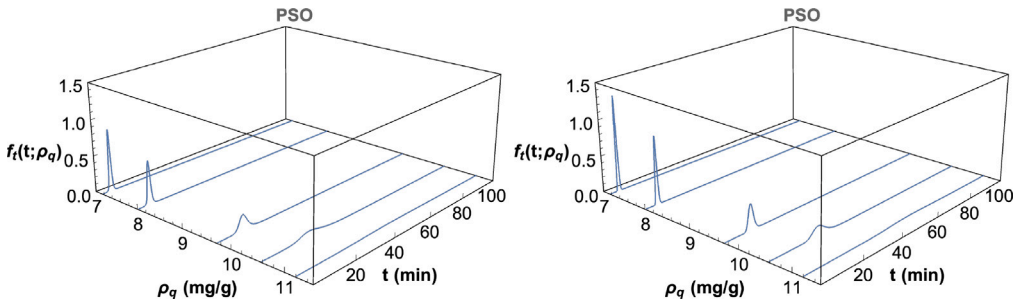


**Fig. 6.** PDF of the time, $f_t(t;\rho_q)$, for different fixed values of the adsorbed amount of reactant $\rho_q \in \{7.172, 8.023, 9.724, 10.575, 11.195\}$. Calculations have been carried out with the PDFs of the model parameters, $k_2(\omega)$ and $q_e(\omega)$, obtained via the Bayes (left) and the RLMS (right) methods, in the context of the PSO model.

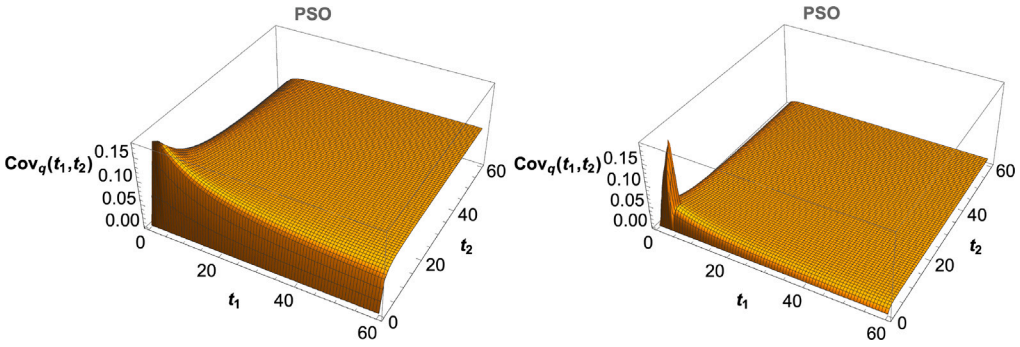


**Fig. 7.** Graphical representation of covariance function of the solution stochastic process of the random PSO model, $\mathrm{Cov}_q(t_1,t_2)$, given in Eqs. (26)–(28), at the time instants $t_i$, $i = 1, 2, \ldots, 9$, collected in Table 1. Left: The PDF of model parameters has been obtained using the Bayesian method. Right: The PDF of model parameters has been obtained using the RLMS method.

**Table 10**
Expectations ($\mu_q(t)$) and standard deviations ($\sigma_q(t)$) of the solution stochastic process of the random PSO model at every time instant, for both Bayes and RLMS approaches.

| | | $t = 4$ | $t = 5$ | $t = 10$ | $t = 15$ | $t = 20$ | $t = 30$ | $t = 45$ | $t = 60$ |
|---|---|---|---|---|---|---|---|---|---|
| Bayes | $\mu_q(t)$ | 7.3777 | 7.9511 | 9.4272 | 10.0510 | 10.3952 | 10.7643 | 11.0256 | 11.1611 |
| | $\sigma_q(t)$ | 0.390147 | 0.370661 | 0.302418 | 0.271691 | 0.256937 | 0.244843 | 0.239724 | 0.238489 |
| RLMS | $\mu_q(t)$ | 7.3233 | 7.9086 | 9.4145 | 10.0532 | 10.4064 | 10.7853 | 11.0538 | 11.1932 |
| | $\sigma_q(t)$ | 0.219735 | 0.208422 | 0.164517 | 0.142718 | 0.131562 | 0.121818 | 0.117275 | 0.115966 |

**Table 11**
Probability, $\mathbb{P}[C]$, of the event $C = \{\omega \in \Omega : q_e(\omega) - \rho_q > 0\}$ calculated in the context of the random PSO model, on the probability space $(\Omega, \mathcal{F}_\Omega, \mathbb{P})$. Expectation, $\mathbb{E}[t(\omega)|C]$, and variance, $\mathbb{V}[t(\omega)|C]$, of the time until a given amount of adsorbed amount of reactant, $\rho_q$, is reached. All the information has been calculated using the Bayes and RLMS approaches for different prefixed values of the chemical concentration, $\rho_q$.

| | $\rho_q \longrightarrow$ | 7.172 | 8.023 | 9.724 | 10.575 | 11.195 |
|---|---|---|---|---|---|---|
| $\mathbb{P}[C]$ | Bayes | 0.999791 | 0.999791 | 0.999600 | 0.997797 | 0.953805 |
| | RLMS | 1 | 1 | 1 | 1 | 1 |
| $\mathbb{E}[t(\omega)\|C]$ | Bayes | 3.74 | 5.19 | 12.17 | 25.14 | 80.33 |
| | RLMS | 3.80 | 5.25 | 12.06 | 23.86 | 65.81 |
| $\mathbb{V}[t(\omega)\|C]$ | Bayes | 0.30 | 0.61 | 5.93 | 68.46 | 4828.12 |
| | RLMS | 0.09 | 0.19 | 1.37 | 10.52 | 616.54 |

knowing if the stochastic process has properties such as stationarity, that play a key role in many applications.

To determine an explicit expression to the 2-PDF of the solution stochastic process, $q(t,\omega)$, of the PSO model, we fix $t_1, t_2 > 0$ being $t_1 \neq t_2$. Without loss of generality, we will assume that $t_1 < t_2$. Now, we will apply Theorem 1 using the following mapping $\mathbf{r} : \mathbb{R}^2 \to \mathbb{R}^2$ as

$$v_1 = r_1(k_2, q_e) = q(t_1) = \frac{k_2 q_e^2 t_1}{1 + k_2 q_e t_1},$$
$$v_2 = r_2(k_2, q_e) = q(t_2) = \frac{k_2 q_e^2 t_2}{1 + k_2 q_e t_2}.$$

Isolating both $k_2$ and $q_e$, we obtain the inverse mapping of $\mathbf{r}$, $\mathbf{s} : \mathbb{R}^2 \to \mathbb{R}^2$,

$$k_2 = s_1(v_1, v_2) = \frac{-(t_1 v_2 - t_2 v_1)^2}{t_1 t_2 (t_2 - t_1) v_1 (v_1 - v_2) v_2},$$
$$q_e = s_2(v_1, v_2) = \frac{(t_1 - t_2) v_1 v_2}{t_1 v_2 - t_2 v_1}.$$

The absolute value of the Jacobian of the inverse mapping $\mathbf{s}$ is

$$|J| = \left| \frac{\partial s_1}{\partial v_1} \frac{\partial s_2}{\partial v_2} - \frac{\partial s_1}{\partial v_2} \frac{\partial s_2}{\partial v_1} \right| = \left| \frac{t_2 - t_1}{t_1 t_2 (v_1 - v_2)^2} \right| \neq 0.$$

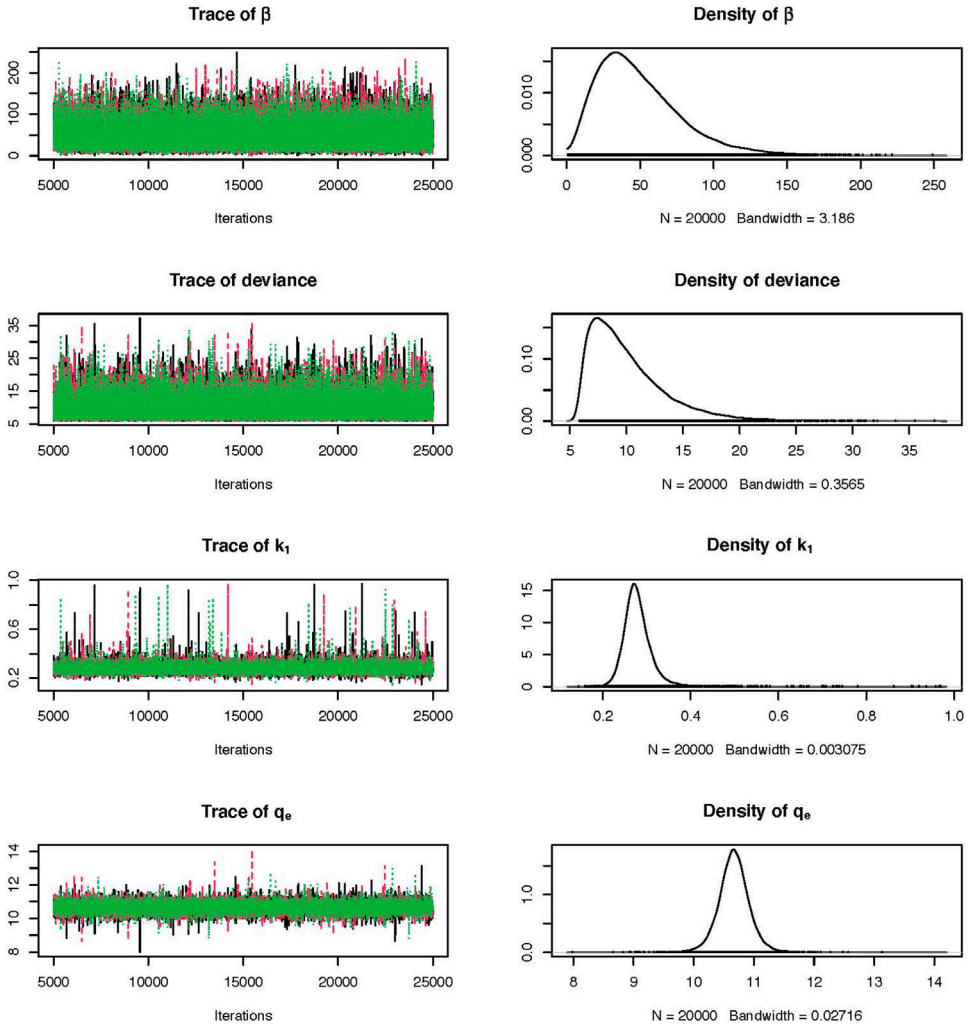


**Fig. A.8.** MCMC trace plot (left column) and marginal posterior distribution (right column) of the samples for the model parameters, $k_1(\omega)$, $q_e(\omega)$, the rate parameter of Gamma distribution, $\beta(\omega)$, and the deviance. This corresponds to PFO model.

Notice that the inverse mapping is well defined since $t_1 \neq t_2$ entails $v_1 \neq v_2$. Then, the joint PDF of the random vector $(v_1(\omega), v_2(\omega))$ is

$$f_{v_1,v_2}(v_1, v_2) = f_0^2\left(\frac{-(t_1v_2 - t_2v_1)^2}{t_1t_2(t_2 - t_1)v_1(v_1 - v_2)v_2}, \frac{(t_1 - t_2)v_1v_2}{t_1v_2 - t_2v_1}\right)\left|\frac{t_2 - t_1}{t_1t_2(v_1 - v_2)^2}\right|,$$

or equivalently, the 2-PDF of the solution stochastic process is

$$f_2(q_1, t_1; q_2, t_2) = f_0^2\left(\frac{-(t_1q_2 - t_2q_1)^2}{t_1t_2(t_2 - t_1)q_1(q_1 - q_2)q_2}, \frac{(t_1 - t_2)q_1q_2}{t_1q_2 - t_2q_1}\right)\left|\frac{t_2 - t_1}{t_1t_2(q_1 - q_2)^2}\right|, \quad (28)$$

for $t_1 \neq t_2$. In Fig. 7, we have plotted the covariance function $\mathrm{Cov}_q(t_1, t_2)$ of the solution stochastic process of PSO model using the parameters distributions of models parameters calculated by the Bayes and the RLMS methods. Let us remember that the variance can be obtained from the covariance function by taking $t_1 = t_2$, so, it is identified with the diagonal of the covariance surface. From the plot, we can observe that, the Bayesian method gives a higher value than the RLMS method, being both constant as $t$ increases, all these features are in full agreement with the analysis performed previously. From both plots, we observe that the covariance is always positive, and approximately constant as $t_1$ and $t_2$ increase, being higher in the case that the Bayesian approach has been applied.

## 4. Conclusions

In this paper, we have proposed the full randomization of two widely used kinetic models, formulated via differential equations, to describe the chemical adsorption process. The novelty of our proposal is that model parameter are treated as random variables rather than deterministic constants. As a consequence, both models are reformulated by random differential equations. We then solve both models probabilistically by determining their respective first probability density functions, which is advantageous with respect to the classical approach, since it permits probabilistically determining relevant information about the chemical process. A strength point in the theoretical analysis is its generality since all the results have been obtained assuming arbitrary distributions for the model parameters. Besides, we have faced an important challenge when random differential equations are applied to real data, namely, how to determine reasonable probability distributions for the model parameters. We have shown two methods to answer this inverse problem, and we have compared the results obtained for the two models. At this point, it is important to point out that this is a critical step in the process of uncertainty quantification when dealing with real-world models since the choice of appropriate distributions is, in general, not unique. In our case, we have validated our results by means of goodness-of-fit measures for two methods applied. Although we have obtained satisfactory results, it must be also remarked the limitations of our approach. First, it has relied on the

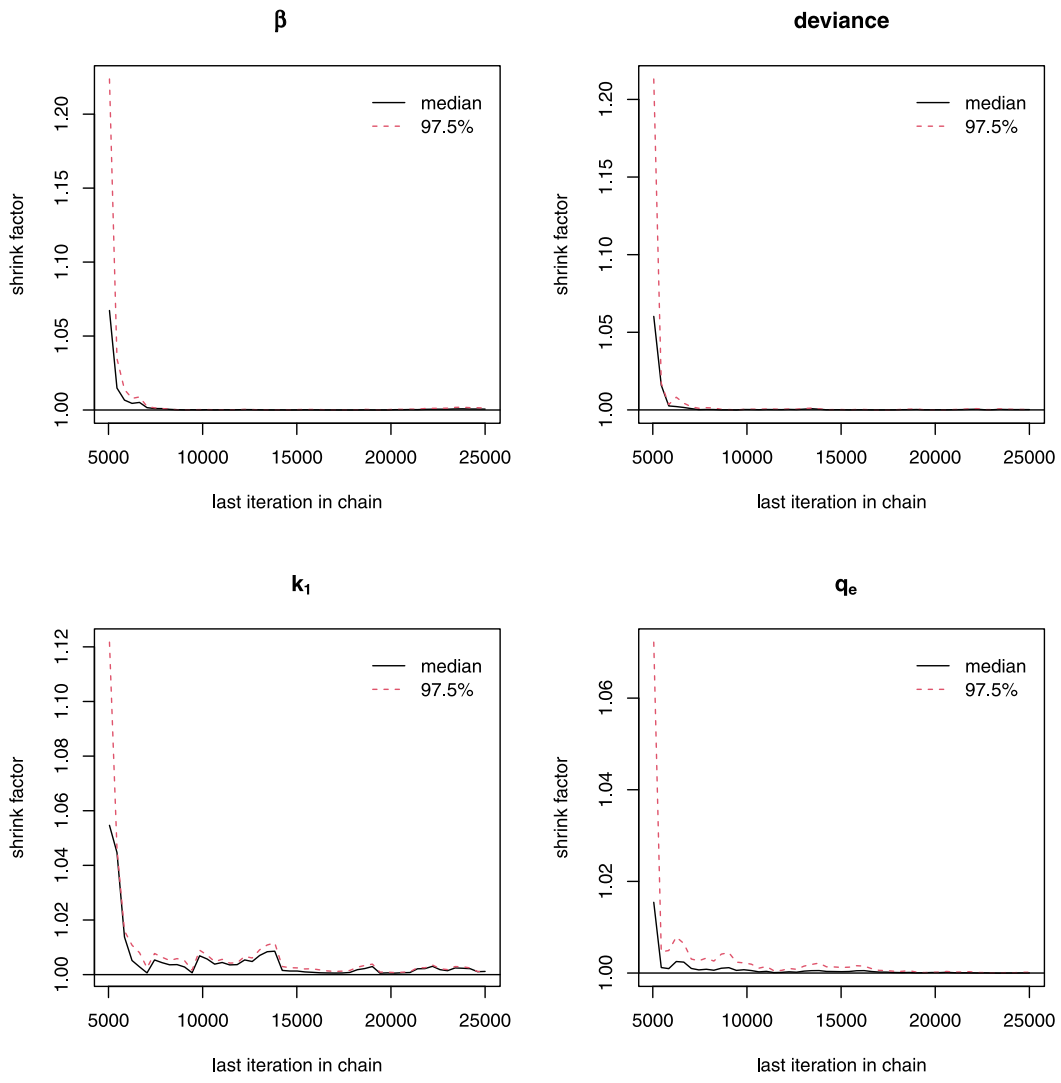


**Fig. A.9.** Gelman and Rubin convergence diagnostic plots, calculated by three Markov chains, for the model parameters, $k_1(\omega)$, $q_e(\omega)$, the rate parameter of Gamma distribution, $\beta(\omega)$, and the deviance. This corresponds to PFO model.

application of the Random Variable Transformation method, which has depended on the knowledge of explicit expressions for the solutions of the PFO and PSO models as well as the definition of an appropriate multidimensional invertible mapping whose inverse and Jacobian are calculable. Albeit the two randomized models analyzed throughout the paper are mathematically simple, we think that the results obtained can be useful to provide more realistic answers to applied problems as well as can open new avenues to study other randomized kinetic models in Chemistry.

## CRediT authorship contribution statement

**J.-C. Cortés:** Conceptualization, Methodology, Validation, Investigation, Writing – review & editing, Supervision, Funding acquisition. **A. Navarro-Quiles:** Conceptualization, Methodology, Software, Validation, Investigation, Writing – original draft, Supervision. **F.-J. Santonja:** Conceptualization, Methodology, Validation, Investigation. **S.-M. Sferle:** Software, Validation, Formal analysis, Investigation, Resources, Data curation, Writing – original draft.

## Declaration of competing interest

The authors declare the following financial interests/personal relationships which may be considered as potential competing interests: Juan Carlos Cortes Lopez reports financial support was provided by Spanish Agencia Estatal de Investigación. Sorina Madalina Sferle reports financial support was provided by Spanish Agencial Estatal de Investigación.

## Data availability

The data were retrieved from available literature as indicated in the paper.

## Acknowledgments

This work has been supported by the grant PID2020-115270GB–I00 granted by MCIN/AEI/10.13039/501100011033 and the grant PRE2021-101090, granted by MCIN/AEI/10.13039/501100011033 and by FSE+. We thank the two anonymous reviewers for their comments that have helped us to improve the paper.

## Appendix. Graphical representation used in the Bayesian parameter estimation technique

See Figs. A.8–A.13.

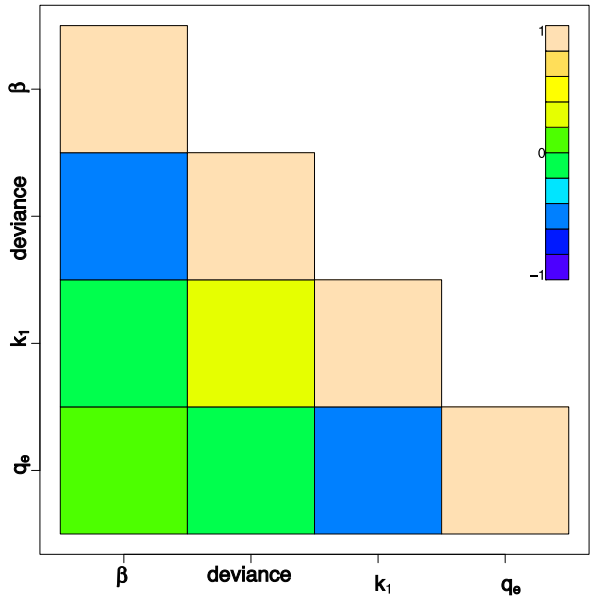


**Fig. A.10.** Cross-correlation plot for the model parameters, $k_1(\omega)$, $q_e(\omega)$, the rate parameter of Gamma distribution, $\beta(\omega)$, and the deviance. This corresponds to PFO model.

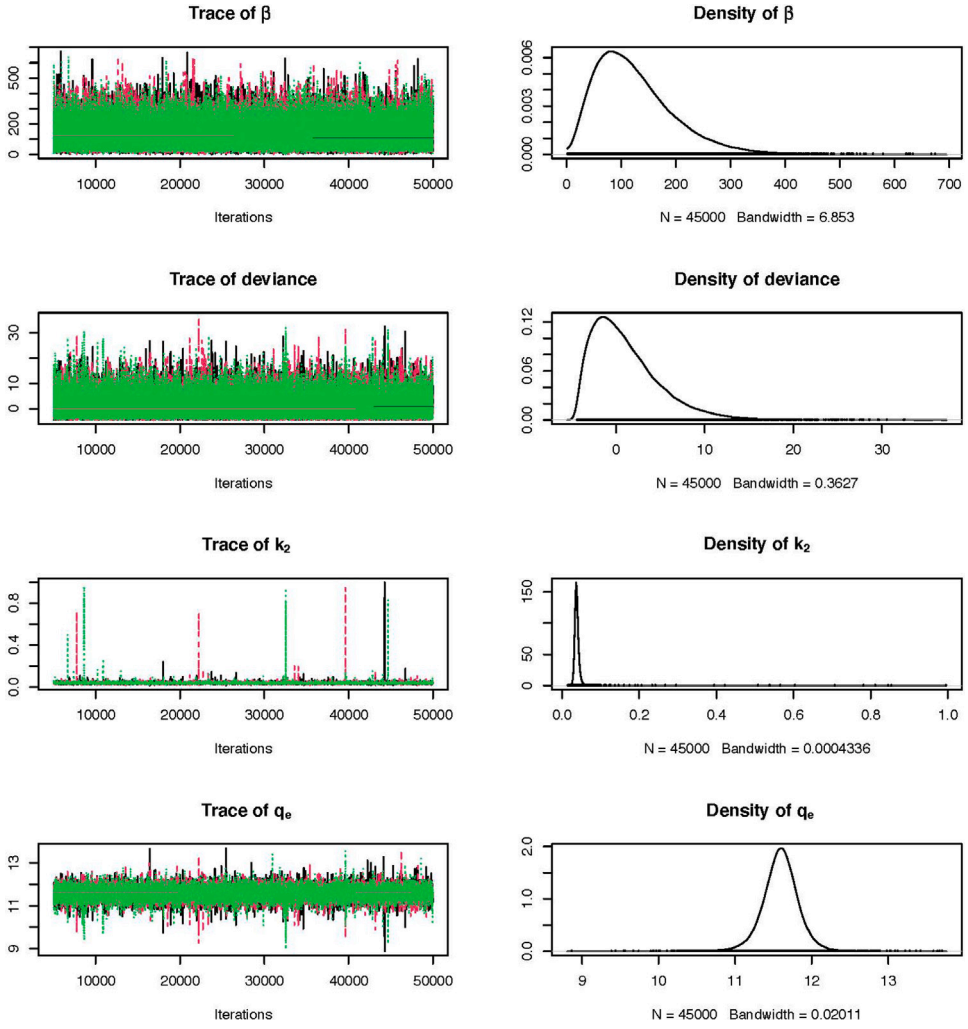


**Fig. A.11.** MCMC trace plot (left column) and marginal posterior distribution (right column) of the samples for the model parameters, $k_2(\omega)$, $q_e(\omega)$, the rate parameter of Gamma distribution, $\beta(\omega)$, and the deviance. This corresponds to PSO model.

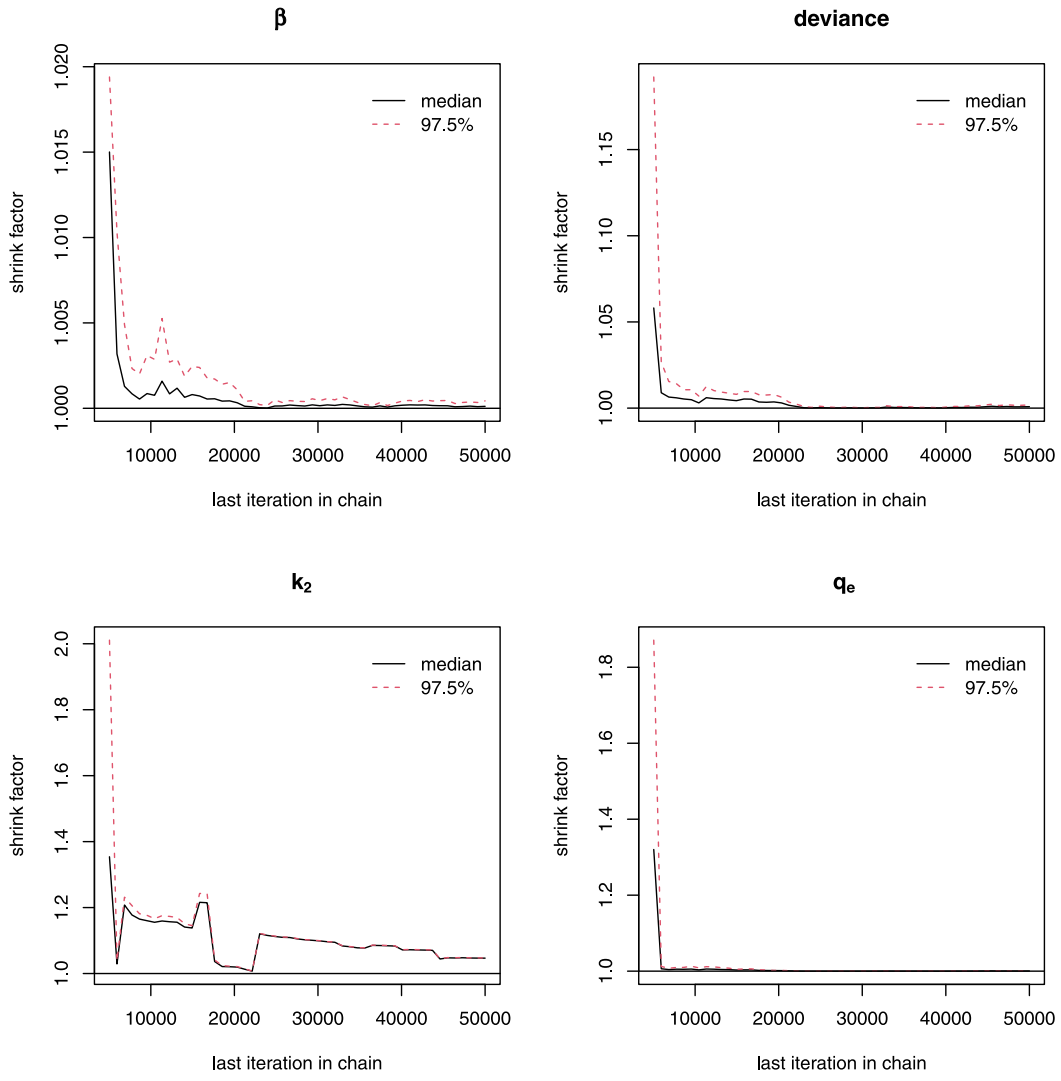


**Fig. A.12.** Gelman and Rubin convergence diagnostic plots, calculated by three Markov chains, for the model parameters, $k_2(\omega)$, $q_e(\omega)$, the rate parameter of Gamma distribution, $\beta(\omega)$, and the deviance. This corresponds to PSO model.

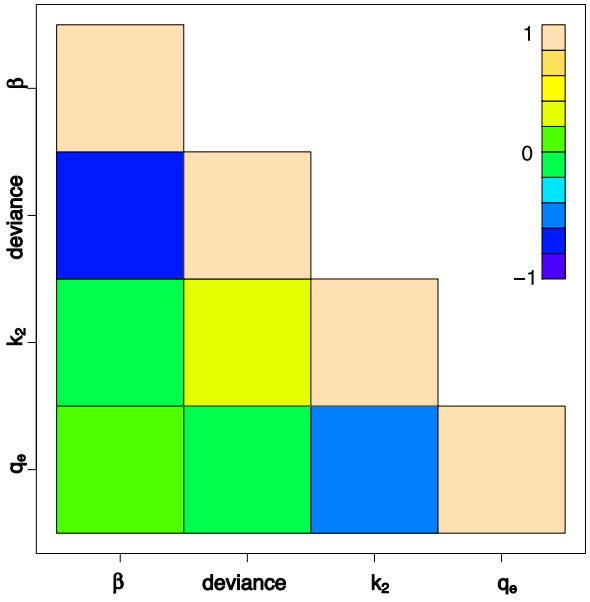


**Fig. A.13.** Cross-correlation plot for the model parameters, $k_2(\omega)$, $q_e(\omega)$, the rate parameter of Gamma distribution, $\beta(\omega)$, and the deviance. This corresponds to PSO model.

## References


[1] S. Glasstone, D. Lewis, Elements of Physical Chemistry, Macmillan Press, London, 1983.

[2] K. Kamalanand, P. Mannar Jawahar, Mathematical Modelling of Systems and Analysis, PHI Learning, Delhi, 2019.

[3] B.L. Granovsky, T. Rolski, W.A. Woyczynski, J.A. Mann, A general stochastic model of adsorption-desorption: Transient behavior, Chemometr. Intell. Lab. Syst. 6 (1989) 273–280.

[4] M. Bouhedda, S. Lefnaoui, S. Rebouh, M.M. Yahoum, Predictive model based on adaptive neuro-fuzzy inference system for estimation of cephalexin adsorption on the octenyl succinic anhydride starch, Chemometr. Intell. Lab. Syst. 193 (2019) 103843.

[5] I.C. Afolabi, S.I. Popoola, O.S. Bello, Modeling pseudo-second-order kinetics of orange peel-paracetamol adsorption process using artificial neural network, Chemometr. Intell. Lab. Syst. 203 (2020) 104053.

[6] I. Ali, G. Gupka, Advances in water treatment by adsorption technology, Nat. Protoc. 1 (2006) 2661–2667.

[7] G. Dotto, G. Mckay, Current scenario and challenges in adsorption for water treatment, J. Environ. Chem. Eng. 8 (2020) 103988.

[8] S. Faust, M. Aly, Adsorption Processes for Water Treatment, Butterworth, 1987.

[9] Y. Zha, Y. Wang, S. Liu, S. Liu, Y. Yan, H. Jiang, Y. Zhang, H. Wang, Adsorption characteristics of organics in the effluent of ultrashort SRT wastewater treatment by single-walled, multi-walled, and graphitized multi-walled carbon nanotubes, Nat. Sci. Rep. 8 (2018) 17245.

[10] Y. Ho, G. McKay, Sorption of dye from aqueous solution by peat, Chem. Eng. J. 70 (1998) 115–124.

[11] S. Lagergren, Zur Theorie Der Sogenannten Adsorption Geloster Stoffe, Kungliga Svenska Vetenskapsakademiens, Handlingar, 1898.

[12] N. Akbar, N. Kamil, N. Zin, M. Adlan, H. Aziz, Assessment of kinetic models on fe adsorption in groundwater using high-quality limestone, IOP Conf. Ser. Earth Environ. Sci. 140 (2018) 012030.
[13] W.-R. Lim, S. Kim, C.-H. Lee, E.-K. Choi, M. Oh, S. Seo, H.-J. Park, S.-Y. Hamm, Performance of composite mineral adsorbents for removing Cu, Cd, and Pb ions from polluted water, Nat. Sci. Rep. 9 (2019) 12598.
[14] H. Moussout, H. Ahlafi, M. Aazza, H. Maghat, Critical of linear and nonlinear equations of pseudo-first order and pseudo-second order kinetic models, Karbala Int. J. Modern Sci. 4 (2018) 244–254.
[15] E. Piperopoulos, L. Calabrese, E. Mastronardo, C. Milone, E. Proverbio, Carbon-based sponges for oil 8 spill recovery, Carbon Nanomater. Agri-Food Environ. Appl. (2020) 155–175.
[16] A.C. Atkinson, B. Bogacka, Compound and other optimum designs for systems of nonlinear differential equations arising in chemical kinetics, Chemometr. Intell. Lab. Syst. 61 (2002) 17–33.
[17] E. Revellame, D. Fortela, W. Sharp, R. Hernandez, M. Zappi, Adsorption kinetic modeling using pseudo-first order and pseudo-second order rate laws: A review, Clean. Eng. Technol. 1 (2020) 100032.
[18] D.O. Hayward, B.M.W. Trapnell, Chemisorption, Butterworths London, 1964.
[19] T. Oden, R. Moser, O. Ghattas, Computer predictions with quantified uncertainty, Part I, SIAM News 43 (2010) 1–3.
[20] A. Der Kiureghian, O. Ditlevsen, Aleatory or epistemic? Does it matter? Struct. Saf. 31 (2009) 105–112.
[21] R. Smith, Uncertainty Quantification: Theory, Implementation, and Applications, SIAM, New York, 2014.
[22] P.E. Kloeden, E. Platen, Numerical Solution of Stochastic Differential Equations, 3th, in: Applications of Mathematics: Stochastic Modelling and Applied Probability, vol. 23, Springer, New York, 1999.
[23] D. Gillespie, A general method for numerically simulating the stochastic time evolution of coupled chemical reactions, J. Comput. Phys. 22 (1976) 403–434.
[24] D. Gillespie, Exact stochastic simulation of coupled chemical reactions, J. Phys. Chem. 81 (1976) 2340–2361.
[25] D. Gillespie, Approximate accelerated stochastic simulation of chemically reacting systems, J. Phys. Chem. 115 (2001) 1716–1733.
[26] S. Rodríguez-Narciso, J. Lozano-Álvarez, Salinas-Gutiérrez, N. Castañeda-Leyva, A stochastic model for adsorption kinetics, Adsorption Sci. Technol. (2021) 5522581.
[27] C. Xu, Threshold dynamics of a stochastic Keizer's model with stochastic incidence, J. Math. Chem. 55 (2017) 1034–1045.
[28] X. Han, P. Kloeden, Random Ordinary Differential Equations and their Numerical Solution, Springer Nature, New York, 2017.
[29] H. Banks, H. Shuhua, W.C. Thompson, Modeling and Inverse Problems in Presence of Uncertainty, CRC Press, Boca Raton, Florida, 2014.
[30] T.T. Soong, Random Differential Equations in Science and Engineering, Academic Press, New York, 1973.
[31] J.-C. Cortés, A. Navarro-Quiles, J. Romero, M. Roselló, Introducing randomness in the analysis of chemical reactions: An analysis based on random differential equations and probability density functions, Comput. Math. Methods 3 (2021) 1–10.
[32] J.-C. Cortés, A. Navarro-Quiles, J. Romero, M. Roselló, A full probabilistic analysis of a randomized kinetic model for reaction–deactivation of hydrogen peroxide decomposition with applications to real data, J. Math. Chem. 59 (2021) 1479–1497.
[33] Y. Ho, Second-order kinetic model for the sorption of cadmium onto tree fern: A comparison of linear and non-linear methods, Water Res. 40 (2006) 119–125.
[34] A. Gelman, J.B. Carlin, H.S. Stern, D.B. Dunson, A. Vehtari, D.B. Rubin, Bayesian Data Analysis. Third Edition, Chapman and Hall/CRC, 1995.
[35] G. Kajjumba, S. Emik, A. Öngen, K. Özcan, S. Aydı n, Modelling of Adsorption Kinetic Processes—Errors, Theory and Application. Chapter in: Advanced Sorption Process Applications, IntechOpen, 2018.
[36] D. Lunn, A. Thomas, N. Best, D. Spiegelhalter, WinBUGS — a Bayesian modelling framework: concepts, structure, and extensibility, Stat. Comput. 10 (2000) 325–337.
[37] S. Sturtz, U. Ligges, A. Gelman, R2WinBUGS: A package for running WinBUGS from R, J. Stat. Softw. 12 (2005) 1–16.
[38] I. Ntzoufras, Bayesian Modeling using WinBUGS, vol. 698, John Wiley and Sons, 2011.
[39] A. Gramacki, Nonparametric Kernel Density Estimation and Its Computational Aspects, in: Studies in Big Data, vol. 37, Springer, 2018.
[40] R. Nelsen, An Introduction to Copulas, in: Lecture Notes in Statistics, vol. 139, Springer, New York, 1999.
[41] S. Sriboonchitta, V. Kreinovich, Why are FGM copulas successful? A simple explanation, Adv. Fuzzy Syst. 2018 (2018) 5872195.
[42] Wolfram Research Inc., Mathematica, version 12.0, 2021, URL https://www.wolfram.com/mathematica, Champaign, IL.
[43] J. Wang, X. Guo, Adsorption kinetic models: Physical meanings, applications, and solving methods, J. Hard Mater. 390 (2020) 122156.
[44] X. Guo, J. Wang, A general kinetic model for adsorption: theoretical analysis and modeling, J. Mol. Liq. 288 (2019) 111100.